SELF-ASSEMBLED SYNTHESIS OF MICROFLUIDIC CHANNELS IN PDMS

by

JEYANTT SRINIVAS SANKARAN

Presented to the Faculty of the Graduate School of

The University of Texas at Arlington in Partial Fulfillment

of the Requirements

for the Degree of

MASTER OF SCIENCE IN ELECTRICAL ENGINEERING

THE UNIVERSITY OF TEXAS AT ARLINGTON

August 2011

ACKNOWLEDGEMENTS

I would like to take this opportunity to express my sincere and heartfelt gratitude to my Professor and thesis advisor Dr. Samir M. Iqbal. His patience during my learning period, guidance, mentorship and the long hours that he spent with me during the research, his insights and help, made this work possible.

I would also like to thank the professors in my thesis committee for their encouragement, enthusiasm and support.

I would like to take this moment to thank the Nanofab and the CCMB staff for their help, suggestions and guidance.

I would like to thank my fellow lab mates who with their questions, comments and discussions helped me mold my thesis. Special thanks to Azhar Ilyas, Motassim Bellah, Nahum Torres, Uyen Pham, Waseem Asghar and Wintana Kahsai for their advice and support.

Lastly and most importantly, I would like to thank my parents for their emotional support, guidance, enthusiasm, encouragement and love.

July 11, 2011

ABSTRACT

SELF-ASSEMBLED SYNTHESIS OF MICROFLUIDIC CHANNELS IN PDMS

Jeyantt Srinivas Sankaran, MS.

The University of Texas at Arlington, 2011

Supervising Professor: Samir M. Iqbal

The field of microfluidics is expanding rapidly finding applications in diverse areas ranging from solid state devices and semiconductors to bio-applications in cell culture and Deoxyribonucleic acid (DNA) assays and micro-arrays. Polydimethylsiloxane (PDMS) has been a commonly used material for the fabrication of microfluidic devices. Apart from traditional lithographic techniques, soft lithography has also been prevalent in fabrication of micro channels in polymers like PDMS. We propose a novel technique for fabrication of micro/nanochannels in PDMS using hydrophilic-hydrophobic interactions. Several hydrophilic materials have been tried for the fabrication of such channels. This research revolves around the science behind the phenomenon, the interactions at the interface between hydrophobic matrix and the hydrophilic material, the thermodynamics involved and the behavior of the micro/nano particles inside a polymer matrix. Iron-oxide nanoparticles and polyurethane beads have been employed before for the fabrication of such devices. We have now introduced Poly ethylene oxide (PEO) as the hydrophilic material in the fabrication of micro/nano channels in PDMS using hydrophobic-hydrophilic interactions. The introduction of PEO for this novel technique of micro/nano channel fabrication provides ease of handling, better inherent

alignment and excellent repeatability. One of the remarkably consistent results of the experiment was the tapered structure of the channels obtained. These channels were closed from both the top and the bottom. Thin layers of PDMS membranes were sliced in order to create ‘through’ channels. It was observed that the slicing of the PDMS provided us with channels whose dimensions can be approximated to be cylindrical. These cylindrical *‘through’ channels* have been shown to act as membranes and preliminary studies indicate that these can be used as micro-reactors for protein purification experiments.

TABLE OF CONTENTS

LIST OF ILLUSTRATIONS

CHAPTER 1

INTRODUCTION

Microfluidics has been one of the rapidly growing fields because of its impact in different areas of science. This amazing field deals with confining and analyzing fluid flows within micrometer scale devices or structures [1]. The emergence of microfluidics provides us with the opportunity to minimize the amount of reagents used for chemical reactions, perform reactions at a smaller scale in a smaller volume which reduces the time required for completion of reactions. The microscale reactions occurring within our body, for example reactions and phenomenon associated with blood flow in micro capillaries, thrombus migration in the blood, can be efficiently studied and analyzed in microfluidic channels while these studies might be inaccurate in macroscale simulations [2].

Microfluidic channels can be fabricated with many types of materials, however Polydimethylsiloxane (PDMS) has been the most popularly used substrate for the fabrication of these channels. The factors favoring PDMS over other materials are numerous. Some of its salient characteristics are its chemical and biological inertness. It allows visible light to pass through, which makes it transparent. Moreover, it is permeable to gases and is thermally stable over the entire range of physiological temperatures and beyond [3-5]. These characteristics make PDMS the most preferred polymer for fabrication of microfluidic channels for biomedical applications.

1.1 Objective

The goals of this thesis span the fabrication of circular microchannels using a novel technique and develop the associated theory behind the new fabrication techniques.

1.2 Synopsis of Research Work

The popularity and widespread use of PDMS for various applications stem from the simplicity of handling PDMS. Microfluidic channels have also been fabricated in glass and silicon, but the processes involved in microfabrication of silicon chips usually include optical lithography, are expensive and time consuming. General techniques of microfabrication on PDMS include soft lithography, e-beam lithography, among others [6, 7]. The method of choice for microchannel fabrication has been soft lithography for PDMS substrates. In this, a master is fabricated with the desired feature which serves as a mold for preparing elastomeric stamps on PDMS. These traditional techniques are associated with challenges in terms of cost and time.

To address these issues, we presented a novel technique in Sankaran et al. [8] in which hydrophilic-hydrophobic interactions were used as the basis for the fabrication of self-aligned microchannels in PDMS. The phenomenon associated with the observed mechanism was also defined and justified [8]. Briefly, the polymerization reaction of PDMS is exothermic and is associated with a decrease in entropy of the system. The reaction is also observed to be spontaneous in the forward direction. According to the second law of thermodynamics, the spontaneity of a reaction, when there is a decrease in entropy can be observed only when there is a significantly large increase in enthalpy of the system. We demonstrated that this enthalpy obtained during the polymerization reaction can be utilized for performing useful work.

The channel dimensions (the length and diameter) and the number of channels were found to be dependent on a number of factors like curing temperature, the amount and type of hydrophilic material used, the thickness of PDMS, the method of application of PDMS on the substrate, the time of curing and the ratio of the curing agent. The interdependence between all these factors is complex but this work throws light on some of these fundamental factors. It describes a theoretical basis, the nature of interdependence and the degree of influence of each of these parameters based on experimental observations.

The diameters of channels were analyzed using scanning electron microscope (SEM), confocal and optical microscopes. The diameters of the channels and the dependence of porosity, with respect to the amount of the Polyethylene oxide (PEO) utilized were characterized. The lengths and shapes of the channels with respect to the thickness of the PDMS and the temperature were also analyzed. The ability of the channels to act as membranes was illustrated by passing different percentage solutions of Sodium Dodecyl Sulfate (SDS) through them without any external aid (i.e. the solutions passed through the PDMS membrane without the application of any external magnetic or electric field and without any surface modification on PDMS like hydrophilization). SDS was chosen as a model solution of interest because it is used as a detergent and surfactant in several biological applications [9-12]. The time it took to pass specific amount of SDS solution was recorded. It showed excellent membrane characteristics of the obtained PDMS membranes.

CHAPTER 2

BACKGROUND AND LITERATURE REVIEW

2.1 Microfluidics

In last few years, the field of microfluidics has grown in leaps and bounds. This exciting venture flourished because of the contribution of scientists from numerous fields. Microfluidics is the ability to work with fluid quantities in the range of micro, nano or pico liters inside a structure or device that has dimensions in the micrometer scale. One of the obvious reasons for the interest in this field can be attributed to the potential of enormous number of applications this venture opens. It would be interesting if we tried to trace the origins of this field, the reasons for its ascendency and importance [13].

2.1.1. Origin of Microfluidics

It is a defining notion and is reported by George M. Whitesides that the field of microfluidics has "four parents" [13]. He reports the origins of microfluidics to be chemical analysis, biodefence, molecular biology and microelectronics. Chemical analysis comes first, with micro analytical techniques likes capillary electrophoresis leading the way. A schematic of microfluidic based capillary electrophoresis channel system is shown in Fig. 2.1 [2].

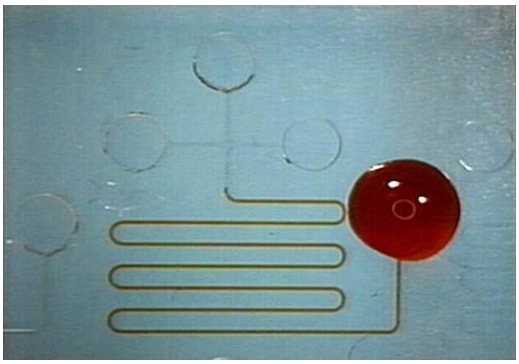

Fig. 2.1 Schematic of a microcapillary electrophoresis test setup with fluid filled channels without cross- talking or cross- linking [14]

These techniques offered tremendous technological and experimental advantages and hence spurred the advances in the field of microfluidics. But as reported in [13] the massive growth of microfluidics began when extensive amounts of funds were invested for biosensing applications by the Defense Advanced Research Projects Agency (DARPA). This investment was stimulated by threats of chemical and biological attacks and to combat new diseases that were emerging during the 1990's. Since then DARPA has been actively funding research for advanced diagnostics, containing toxics, decontamination and medical therapies. Defense Sciences Office (DSO) has extensively funded pioneers for the development of novel diagnostic platforms. This has been the key to widespread growth of microfluidic systems research in universities and other research institutions. The third contributing factor to the growth of microfluidics is the progress in the field of molecular biology, particularly the development of DNA and gene sequencing techniques [15-17]. These required manipulation of fluids at nanoscale volumes in nano/micro sized channels like those shown in figure 2.2. The fourth and the final innovation that stimulated vigorous research in the field of microfluidics was the advancement made in the field of solid-state fabrication of silicon chips. Microarray fabrication on silicon [18, 19], the development of glass based microchannel fabrication [20] and the rise of organic materials [21] for fabrication with the advent of soft lithography, replica molding amongst

other low-cost, high throughput techniques finally established the field of microfluidics as one of the most sought after areas of inter-disciplinary research.

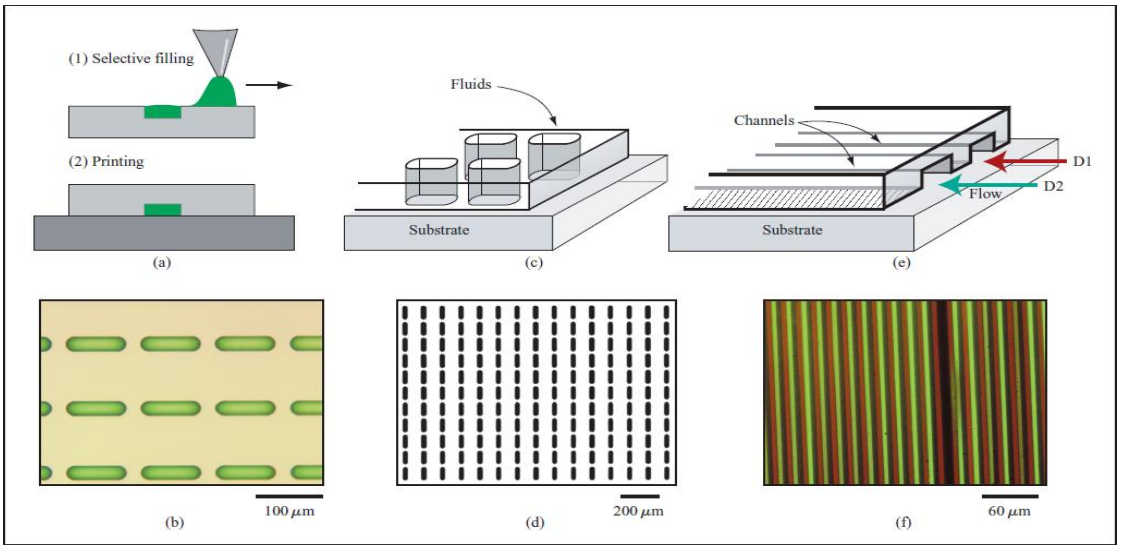

Fig. 2.2 Different microfluidic techniques (a) Cavities in substrates selectively filled with fluids (Writing); (b) Optical micrograph of Polydimethylsiloxane (PDMS) channels filled with dyes; (c) Screen printing technique to localize chemical reactions; (d) Optical micrograph of silicon micro array; (e) Microfluidic channels on a substrate; (f) Fluorescence image of dyes in microfluidic channels [7]

2.1.2. Applications of Microfluidics

Now that we have briefly reviewed the origins of microfluidics, we can now move on to the different areas of research which have flourished after the rise of microfluidics. Research in microfluidics has said to have created three branches of approach. To begin with, the fabrication of microfluidic channels (as discussed in detail in section 2.1.4), then the assembling of small components likes valves and micropumps for the functional applications of microfluidics in complex systems like those shown in Figures 2.3 and 2.4, and finally the study of fluid flow in such systems [22].

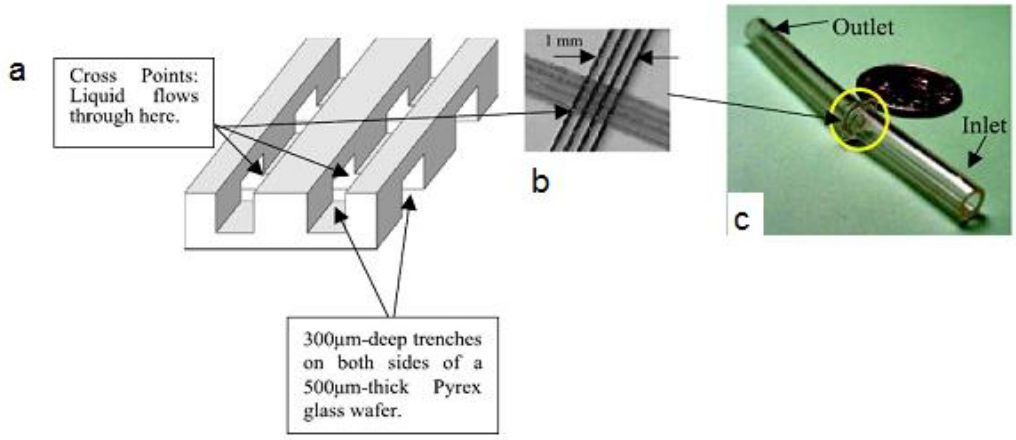

Fig. 2.3 Fluid pumping devices (a) Schematic of a microvalve; (b) Photomicrograph of a microvalve (center); (c) Integration of a microvalve in a test tubing system (right) [23]

The most widely portrayed applications of microfluidics are in the field of biological and chemical studies. But this amazing science, when perfected and mastered, can be applied in several other fields ranging from control systems in electrical and electronic circuits especially in aircrafts, micro-heat sinks or coolant systems for integrated circuits, to the areas of energy generation and display systems. One of the established and well studied applications of microfluidics is inkjet printing. In this, drops of ink are manipulated through openings that have dimensions of the order of a few micrometers to about a 100 µm [22].

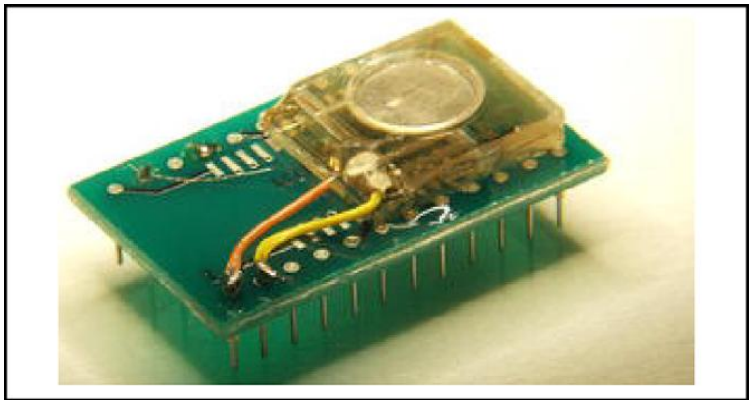

Fig. 2.4 A Microflow controller comprising of a microvalve made of a piezo material and a flow sensor made of a polyimide membrane, all integrated on a printed circuit board [14].

Microfluidics has been employed to a great extent and has showed great promise in the field of biology. Microfluidic systems have been explored for applications ranging from drug delivery vehicles implanted in the body to development of portable diagnostic devices [23], lab-on-chip devices [24], to single cell manipulation [25], detection of microbes and virus (Fig. 2.5), separation of biomolecules by techniques like electrophoresis and dielectrophoresis [26] and also in the fields of microcirculation for simulating blood flow conditions in arteries to study tumor spheroids [27, 28]. The advantages of employing microfluidic systems in these applications are: 1. Reduction in size; 2. Portability and convenience; 3. Rapid fabrication and prototyping; 4. Low cost; 5. Lesser amount of sample and reagent requirement; and 6. Speed and sensitivity of measurement.

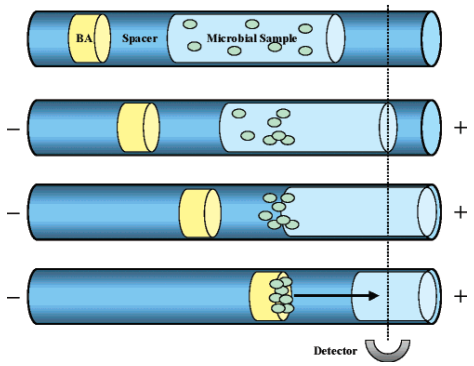

Fig. 2.5 Microcapillary electrophoresis test setup for detection of microbial contamination [29]

2.1.3. Microfluidics and its Associated Physics

We have come across the sections dealing with the inspiration, growth and applications in the field of microfluidics; we could now review some of the basic physics that underlie these devices. One of the important concepts to consider would be the fluid flows inside microfluidic channels. Flow of a liquid inside a micrometer sized channel is normally laminar [1, 30]. That means the fluid flow inside the channel is uniform and its velocity profile does not vary randomly

with time. The Reynolds number of such flow regimes is below 2300. It can be calculated using the formula [1],

$$\mathrm{Re} = \frac{\rho v D_h}{\mu} \qquad (2.1)$$

Where ρ is the density of the fluid, v is the velocity of the fluid, μ is its viscosity and D_h is the hydraulic diameter which is a value based on the geometry of the fluid. Moreover the flow is uniaxial. That is the flow conforms to the topography of the channel walls. Laminar flow often translates into a condition where two different liquids can flow side by side without mixing except by diffusion. This particular phenomenon has been utilized for separation of molecules with respect to their size and this has also been utilized to study motion of cells as they flow through the blood vessels. Diffusion is another process which plays a significant role in microenvironments [1, 30]. It is a process which works towards minimizing the concentration gradient till equilibrium is achieved. It is governed by the equation $d^2 = 2Dt$ where d is the distance to which a particle can diffuse, D is the diffusion coefficient of the particle and t is the time of diffusion. As the dimensions reduce, the time (t) taken for diffusion drops considerably, making it a key factor to be considered. Resistance is also another important factor to be considered both at macro and micro scales. The rate of fluid flow within a microchannel can be calculated as $Q = \frac{\Delta P}{R}$, where Q is the flow rate, ΔP is the difference in pressure and R is the resistance to fluid flow by the walls of the microchannel. The resistance R varies as the channel geometry differs. The resistance offered by circular channels is given by

$$R = \frac{8\mu L}{\pi r^4} \qquad (2.2)$$

where r is the radius of the channel, L is the length of the channel and μ is the fluid viscosity. Another concept that is crucial in microfluidic devices is electro-kinetically induced flows [1, 30]. Electrokinetics is the study of motion of charged particles in a liquid in the presence of an

applied electric field. Electrokinetic flows are further classified as electrophoresis, dielectrophoresis, electro-osmosis and so on [31]. Generally when a polar liquid is in contact with a solid surface, charge is induced on the solid surface because of ionization, ion adsorption or other such effects.

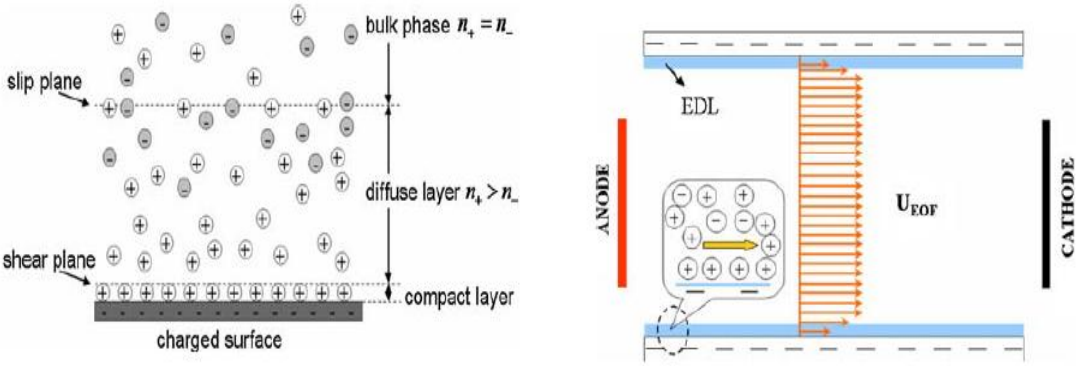

Fig. 2.6 Electrical double layer formation at the surface of a substrate (left) and the electroosmotic flow schematic in the presence of two immersed electrodes inside a liquid (right) [31]

The presence of a charged stationary layer attracts counter-ions from the electrolyte solution in the channel. This leads to the formation of an electrical double layer (EDL). When an electric field is applied tangential to this EDL, charge transport occurs. The charge transport due to phenomena such as viscosity induces mass transport of liquid based on the applied electric field [32]. The formation of EDL and the charge separations in the bulk liquid are illustrated in the figure 2.6 above.

2.1.4. Fabrication of Microfluidic Channels

Fabrication of microfluidic structures is one of the branches of microfluidics that has grown immensely. Several techniques have found way into fabrication based on constraints like cost, speed, know-how, available technology, required resolution and accuracy, application and choice of substrate used. Before the advent of the organic substrates, silicon and glass were the predominantly used substrates for microfluidic channel fabrication. A natural consequence of this was that this field flourished from the fabrication expertise inherited and adapted from the

microelectronic and integrated circuit (IC) fabrication industry [13, 22]. Photolithography and electron beam (e-beam) lithography were the most common techniques used for silicon substrates. Etching techniques like reactive ion etching, wet and dry etching techniques were also employed for the fabrication of microchannels. The advantages of using such techniques are that they have a great deal of accuracy and precision. These produce very high resolution patterns and allow parallel processing. On the downside, these techniques require cleanroom facilities, are expensive, and it is difficult to use conventional biological characterization techniques because Si is not transparent. Glass was subsequently used for fabrication because of its optical properties (mainly transparency) and its well known processing techniques. But the processing of glass is expensive and hence it has not found many takers. Hence the focus moved on to alternate technology in the form of organic polymers that offer excellent optical properties and are more biocompatible for implantable devices [33, 34]. Five different techniques for fabrication of microstructures on organic polymers have been explored [6]. These are micro contact printing (μCP), micro contact molding (μCM), micromolding in capillaries (MIMIC), solvent assisted molding (SAMIM) and replica molding (REM) [6]. All processes involving soft lithography generally make use of the “master” and the “stamp”. A master is a substrate made of metal or Si in which the relief structures are fabricated using photolithography, e-beam lithography or by any other available method. Once a master is obtained, the PDMS stamps are prepared by using the master as the template. The PDMS pre-polymer is poured over the template and is cured. The relief features on the master are transferred on to the stamp. The μCP is a process of forming self assembled monolayers (SAM) on a substrate by coating the stamp with the required molecules and then transferring it by conformal contact with the substrate as shown in the figure below.

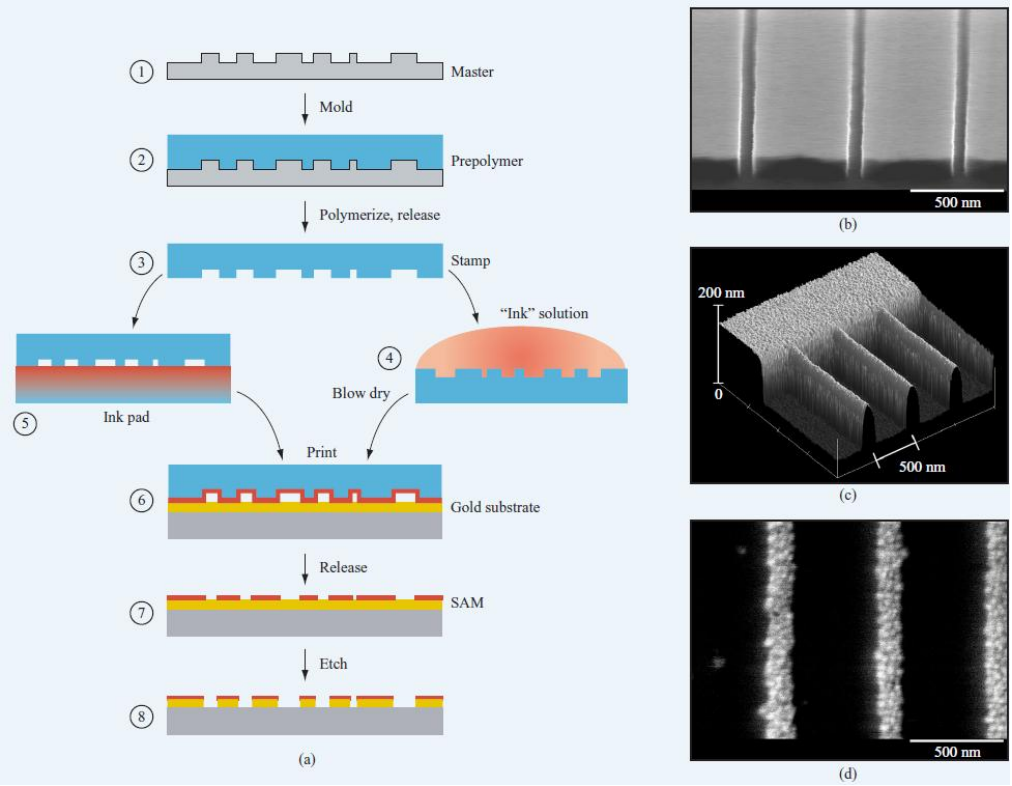

Fig. 2.7 Schematic showing (a) Various steps involved in soft lithography. The fabrication of a master (1), the formation of the stamp (3) by using a pre-polymer over the master (2). The subsequent steps are specific to formation of self assembled monolayers on a substrate by using µCP; (b) SEM micrographs of a master; (c) Stamp; (d) Transferred pattern with the help of the stamp (d) [7]

Replica molding (REM) is a process where a UV or thermally curable pre-polymer, which is not associated with any solvent, is used for the formation of the stamps. This technique is useful for transfer of pattern from a master to a mold and then on to desired substrate with high resolution and hence it is used to print features at the nanometer scale. µTM is a process of fabrication of microchannels. In this method pre-polymer is first poured on the mold and the excess is removed to form a planar surface. It is then placed on a substrate to produce structures as shown in Fig. 2.8. MIMIC is another technique for the fabrication of microchannels where the mold is placed on the substrate and the pre-polymer is placed on one end and it fills the channels by means of capillary action. On curing, structure of channels, complementary to

the pattern in the mold is obtained on the substrate. In SAMIM, a solvent that can dissolve the substrate is used in place of the pre-polymer. When it is placed on the substrate it is selectively in contact with the substrate and results in formation of pattern that is complementary to that on the mold. Fig. 2.9 illustrates one application of microfluidic channels printed using soft lithographic techniques.

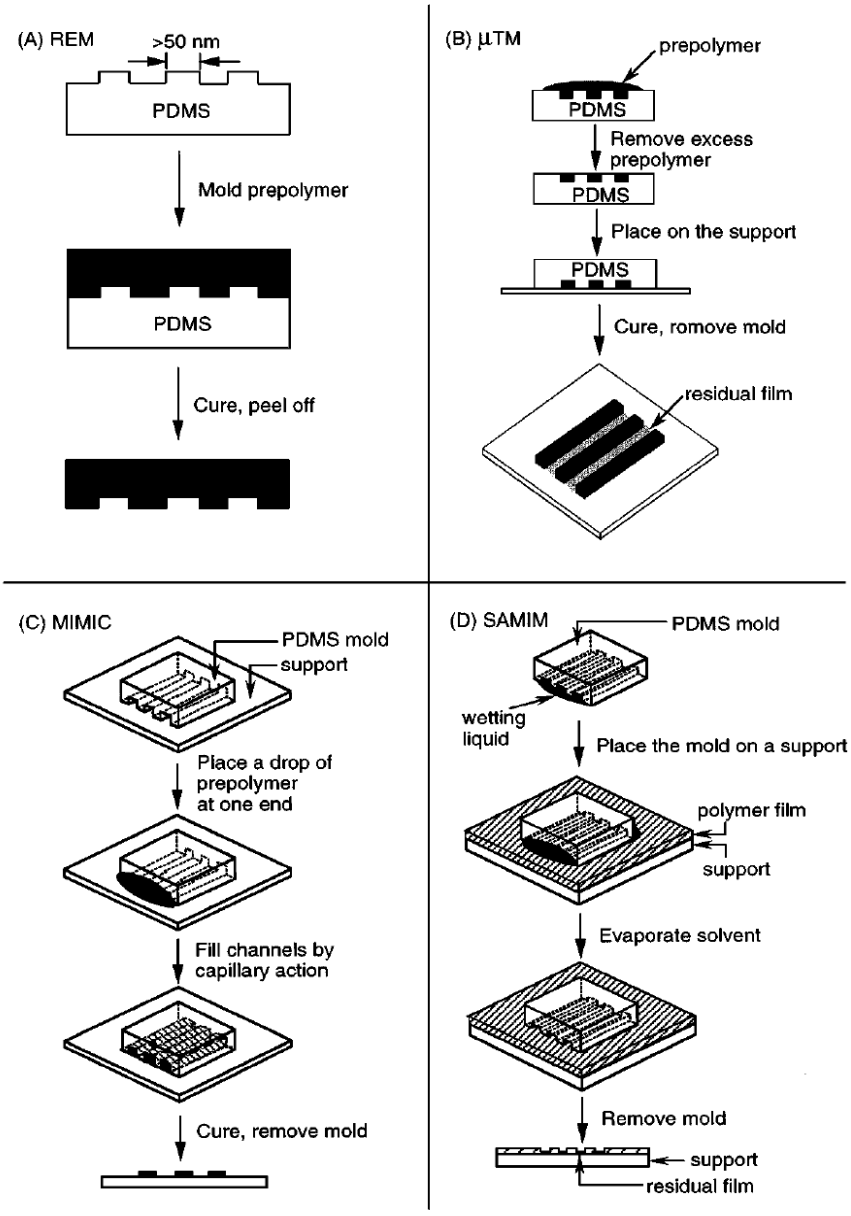

Fig. 2.8 Schematic of different soft lithography approaches detailed under section 2.1.4 [6]

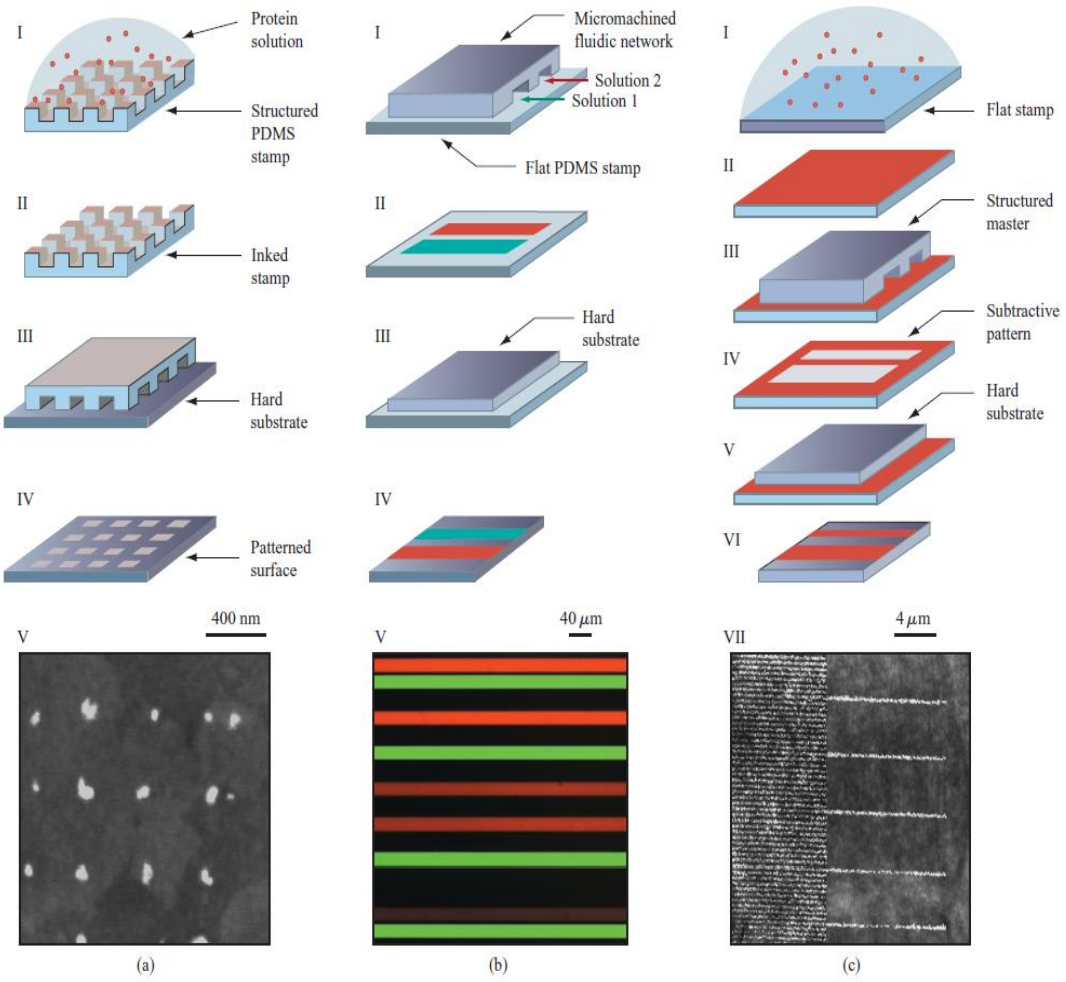

Fig. 2.9 Schematic of soft lithography techniques used for printing biological molecules on a substrate (a), Microfluidic channels and stamps made by printing techniques (b and c). The last image in a, b and c are AFM images showing immunoglobulin printed on glass, sixteen different proteins exhibiting a fluorescent image and 100 nm protein lines respectively [7].

Photolithography is expensive, requires cleanroom facilities and is most suitable only for substrates which are coated with photoresists. Soft lithography is not a single step process. It requires the creation of a master which can normally be fabricated only using the photolithographic methods. For fabrication of simple straightforward microfluidic channels the time consumed is on the higher side. Moreover, the soft lithography techniques frequently in practice often are used to fabricate only rectangular microfluidic channels [6]. Recently a few

techniques have been proposed for fabrication of circular channels. We propose a new technology for the fabrication of circular microfluidic channels in PDMS using hydrophobic-hydrophilic interactions [35]. This fabrication is a single step process and does not involve lithography. The entire process can be completed within an hour, it does not require cleanroom facilities and it is inexpensive.

2.1.5 Fundamental Curing Process of Polymers

A simple approach to create microchannels in PDMS using hydrophobic-hydrophilic interactions has been developed and is the main focus of this thesis. It is based on the principle that the hydrophobic chains of PDMS expel the hydrophilic materials out of its polymer matrix as the polymerization reaction proceeds. This phenomenon has been used to produce microchannels. The process is straightforward, the procedure is systematic, and the substrate is flexible and a wide variety of hydrophilic materials can be used for this process and hence the entire process is flexible, easy to implement, rapid, inexpensive and does not require lithography. When PDMS is subjected to directed thermal curing it undergoes a phase change from liquid to solid. Gel Point (GP) is the time in polymerization reaction when the polymer starts losing its fluidity and starts the process of cross-linking. It can hence be considered that GP is the time when phase transition from a fluidic system to a gel like system occurs. There is a decrease in entropy at this point. When hydrophilic particles are present inside the hydrophobic PDMS matrix, they are pushed out of the PDMS matrix at GP because of the enthalpy that results out of the reduction in free energy. This has been used for the fabrication of microfluidic channels.

2.1.6 Hydrophilic Polymers

Hydrophilic polymers are those polymers that can readily absorb water. These polymers undergo considerable changes in their structure and also in their physical and thermal properties after the absorption of water [36]. Water absorption increases the flexibility of the polymer chains. This in turn reduces the glass transition temperature [37, 38]. These hydrophilic

polymers are employed in a wide variety of applications like improving the hydrophilicity of liposomes to prevent their uptake by the mononuclear phagocyte system (MPS) [39], some hydrophilic polymers are used as an used as an injectable bone substitute [40], they are used to control nutrient release [41], they are used to prevent non specific adsorption of proteins in PDMS [42], and they are used in pervaporation experiments [43, 44].

2.1.7 Hydrophobic Polymers

Hydrophobic polymers are some of the most commonly used class of polymeric materials used for microfluidic applications. Hydrophobic surfaces are presented by hydrophobic polymers and it is more of a surface property rather than the bulk property of the polymer, which comes into play when this phenomenon is exploited for applications. Some of the hydrophobic polymers that are widely in use for fabrication of microfluidic devices are teflon, polystyrene, PDMS and so on [45]. PDMS is reported to be an inert polymer without any reactive groups on the surface. But, experimental data has shown time and again that these polymers have significant surface charge. The origin of such charges and has been discussed earlier in considerable detail. Experimental observations of zeta potential and electro osmotic flow are reported in the next chapter [45].

CHAPTER 3

HYDROPHOBIC-HYDROPHILIC INTERACTIONS IN PDMS

3.1 Theoretical Basis of Fabrication

PDMS is an elastic solid that is widely used in biological sensing-applications because it has favorable optical properties, is flexible and, biologically inert and has a very low glass transition temperature. Moreover, it is permeable to gases and above all, it is easy to fabricate structures in PDMS bulk [6, 46, 47]. PDMS is inherently hydrophobic because of the presence of the repeating siloxane groups in its network structure. This is achieved by the low molar mass PDMS chains migrating to the surface from the bulk of the PDMS[48]. This hydrophobic nature of PDMS has been efficiently utilized in this novel fabrication procedure.

3.1.1. Hydrophobicity

Hydrophobicity, in a very broad sense is the property of apolar molecules that do not have a tendency to dissolve in water. It has been adequately discussed before that hydrophobic interaction strengthens with temperature. Hence they are often considered to be entropic i.e. they induce configurational order in the immediate environment [49, 50].

3.1.2. Hydrophilicity

It is often quoted that hydrophilic materials are those whose surface can be wetted by water. It is also a natural tendency to consider that materials that interact with water and are soluble in the water are called hydrophilic [50]. The definition of hydrophilicity and hydrophobicity when considered as separate entities are purely descriptive and cannot be quantified. To quantify these terms it has to be analyzed thermodynamically and has been stated that when the net free energy of interaction of molecules of a substance is considerably repulsive then the particles can be considered to be hydrophilic [49]. This means that the free

energy of interaction has to be positive. The hydrophilicity is directly proportional to the degree to which the net free energy is positive. In other words when the interfacial attractive forces between the particles are much stronger than the attractive forces toward water, then these are hydrophobic and the net interfacial free energy is positive [51, 52].

3.2 Hydrophobic-Hydrophilic Interaction Studies

3.2.1. General Studies

The interactions observed when hydrophobic particles are suspended in a hydrophilic material or vice versa are exciting and have been well documented. One of the logical outcomes of such reactions is clustering. When we consider hydrophobic particles in a hydrophilic solvent, say water, the interfacial free energy among the particles is positive which implies they are attractive. This leads to clustering of molecules. This can also be explained on the basis of solvation free energy ΔG_{solv}. The value of ΔG_{solv} can be assumed to be the sum of three different free energy parameters: a) the solvation free energy to form a single hydrophobic particle-solvent excluded volume ΔG_{EV}, b) free energy associated with the electrostatic interaction between the hydrophobic particle and water ΔG_{el}, c) the free energy associated with the attractive or repulsive forces (van der Waals force) between the hydrophobic particle and water ΔG_{sr} [53].

$$\Delta G_{solv} = \Delta G_{ev} + \Delta G_{El} + \Delta G_{sr} \qquad (3.1)$$

When the hydrophobic particles do not form clusters and each particle is separately solvated, the solvation free energy grows linearly with every new particle in water. The contributive free energies in the above equation are volume dependent when the particles are dispersed but their dependence is on the combined overall surface area of the cluster when the hydrophobic particles collapse. The free energy is considerably less when the particles collapse and this is thermodynamically more favorable than the dispersed state and hence the particles tend to agglomerate in aqueous solutions. This has been illustrated graphically in figure 1 below [49]. It has also been reported that the force or the intent to form clusters increases with increasing

temperature. This particular phenomenon observed is called the entropy effect. The clustering effect is then said to be induced by the difference in the entropy assisted solvation free energy of the hydrophobic particles and the enthalpy driven solvation free energy of the water molecules. One of the logical conclusions that we can deduce from the above theory is that a true macroscopic hydrophobic surface can never be completely dry because the energy required to move the water molecules to large distances would not be energetically favorable [49].

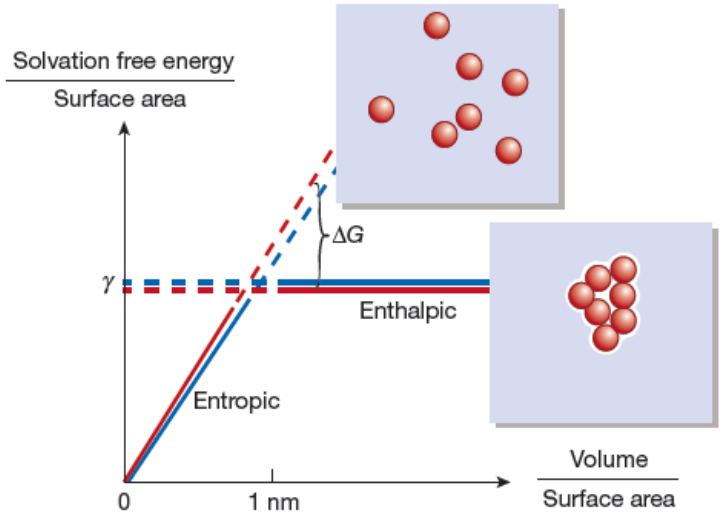

Fig. 3.1 Energy landscape favoring clustering of hydrophobic particles in an aqueous solution [49]

3.2.2. Thermodynamic Basis of Fabrication

It is believed that polymerization reactions are usually exothermic. Exothermic reactions are those reactions where heat is released to the environment. By convention the enthalpy *(∆H)* of such reactions is negative. Endothermic reactions on the other hand absorb heat form the surroundings [8]. Enthalpy can be understood as the potential energy required for the interaction between different monomeric units. It can be represented by the equation,

$$\Delta H = \Delta E - P\Delta V \qquad (3.2)$$

Where ΔE is the change in internal energy, and ΔV id the change in volume associated of the monomeric units associated with the polymerization reaction. For reactions taking place at atmospheric pressure, the $P\Delta V$ term is reported to be negligible. Therefore the change in enthalpy is essentially a change in internal energy of the monomer [54]. Internal energy is the energy (kinetic+potential) of the particles that make up a system. Moreover, internal energy is a state function. That is internal energy of a system is always measured at a specific time. It is a measure of the difference in internal energy between the final and initial state. The internal energy of a system can be defined on the basis of the first law of thermodynamics [55, 56].

$$E = q + W \tag{3.3}$$

where q is the heat absorbed or released and w is the work done on the system or work done by the system. When heat is supplied to a system the sign convention for q and E is positive. That is there is an increase in the internal energy of the system. This can be logically interpreted by considering that increasing the temperature of a macroscopic material, increases the mobility of the ions and this increases the kinetic energy and hence the internal energy. It can also be stated that when work is done by the system on the surroundings, the sign convention is negative. In the case of polymerization reactions, volume change is observed in the system and hence work is done by the system. However the value of $P\Delta V$ has been neglected for polymerization reactions taking place at atmospheric pressure [54, 56].

Polymerization of PDMS is carried out by adding the PDMS base and the curing agent in a specific ratio. The PDMS base and the curing agent are viscous liquids. At high temperatures, polymerization reaction ensues and these liquid pre-cursors form elastic polymer solids. Entropy can be stated as the extent of disorder in a system [49]. Phase change of the polymer from a viscous melt to a solid will lead to a decrease in the entropy. The translational entropy would decrease to a considerable extent. PDMS is flexible and the chains of PDMS in the bulk have been reported to rise to the surface to regain the hydrophobic character of the

surface. This could be extended to say that rotational and vibrational entropy have the ability to compensate for the loss of translational entropy. However, when polymerization reaction results in formation of stable cross-linked structures, the entropy of the PDMS matrix would drop sufficiently to limit both the vibrational and rotational entropy [49]. Entropy is also a state function and can be given by,

$$\Delta S_{reaction} = \Delta S_{products} - \Delta S_{reactants} \quad (3.4)$$

The entropy of the products in the solid phase is much lesser than the entropy of the reactants in the liquid phase, hence the net entropy of the reaction would be negative *(-∆S)*. The phase change ensuing polymerization results in the reduction of the number of configurations that the polymer and this directly leads to a decrease in the entropy of such reactions. The Gibbs free energy *(∆G)* determines the spontaneity of a reaction and is a combination of both the enthalpy and entropy. The Gibbs free energy is related to the enthalpy, entropy and the temperature *(T)* of the system by the following equation,

$$\Delta G = \Delta H - T\Delta S \quad (3.5)$$

When the system consisting of the PDMS base and curing agent inside a beaker is considered to be an isolated system, the reaction proceeds in the direction of polymerization, albeit very slowly. This shows that the reaction is spontaneous and the rate of the reaction can be enhanced to a great extent by providing heat to that system. According to the second law of thermodynamics, a reaction can procced in forward direction when there is such a large decrease in entropy as observed in our system only if there is a sufficiently large change in the internal energy or the enthalpy of the system [57]. We present an approach to utilize this large enthalpy change produced during polymerization to perform useful work in the direction of fabrication of microfluidic channels.

3.3 Experimental Approach

This work demonstrates a technique in which hydrophilic particles are introduced into a system of the uncured PDMS polymer matrix, the tendency of the hydrophobic polymer matrix

has been observed to be to expel the particles out. The hydrophobic polymer matrix has favorable energy orientations when it maintains a minimal interfacial contact with the hydrophilic particles. The energy required for this work is provided when heat is supplied for curing the PDMS matrix in the form of reduced entropy and the subsequent large increase in enthalpy and free energy of the system until equilibrium is achieved by cross-linking.

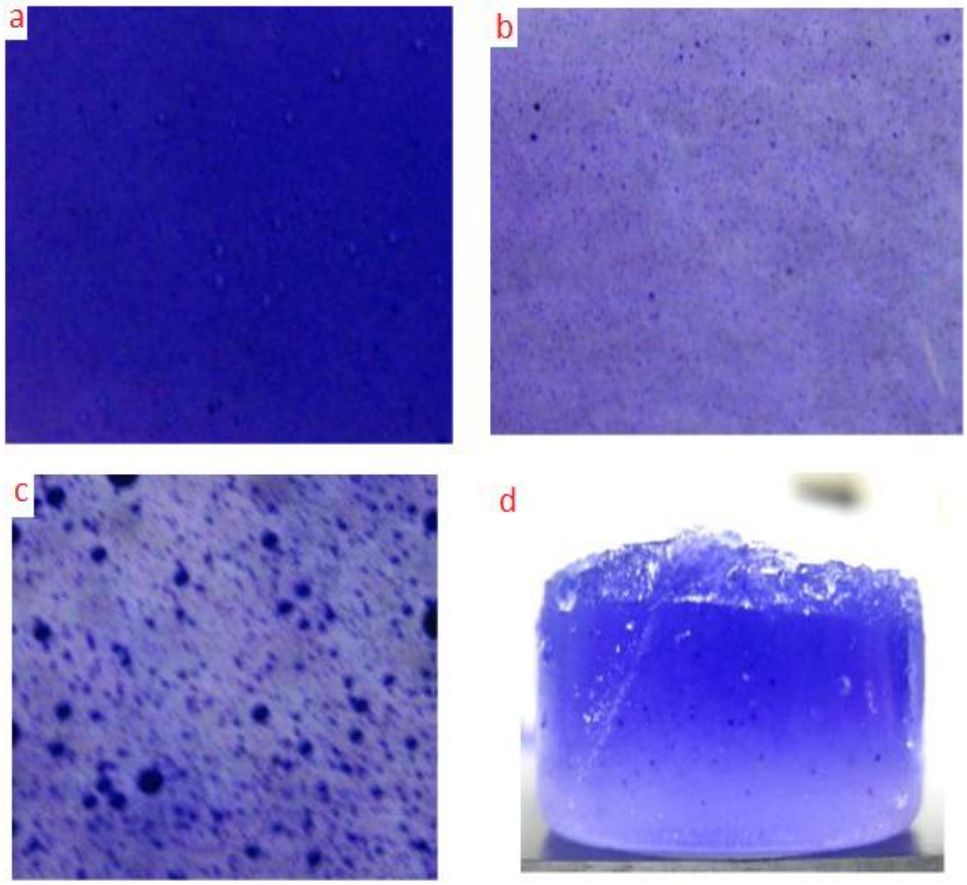

Fig. 3.2 Blue ink in PDMS. Time scope as PDMS polymerizes (a) at time *T*=0, homogeneous mixing of ink in the PDMS precursor (b) At time *T*= 20 min clustering of ink (c) At time *T* = 90 min ink rises through the matrix displaying a gradient (d) The small clusters of ink are pushed out of the PDMS matrix[8]

To demonstrate this phenomenon, ink was mixed with PDMS pre-polymer and was then subjected to curing at elevated temperature. It was observed that the ink droplets rose to the

surface of the PDMS slab (as shown in figure 3.2). The clustering of the ink droplets prior to rising through the matrix was as expected and followed the mechanism discussed in section

3.3.1. Experimental Methods (Polyurethane beads)

Hydrophilic polyurethane beads were used to fabricate self-aligned microfluidic channels. The polyurethane beads (PU), industrially known as 'Tecoflex-EG-80A' was obtained from Lubrizol incorporation had a diameter in the range of 2.5-3.5 mm.

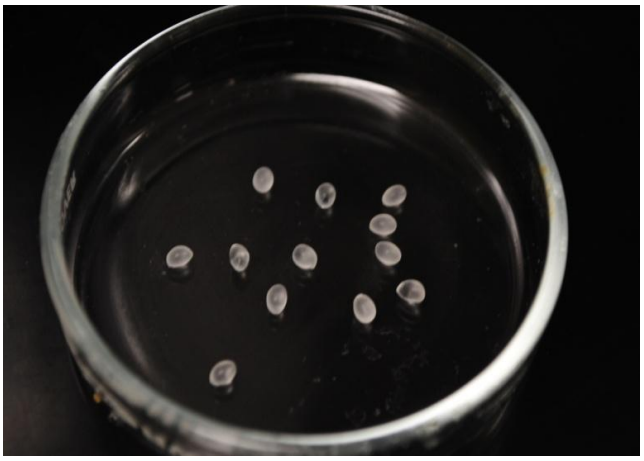

Fig. 3.3 Tecoflex polyurethane beads placed on a Petri dish before subjecting them to heat

The PU beads were placed on the Petri dish. PDMS solution was prepared with the curing agent in the ratio of 10:1 and was introduced on top of the beads in the dish as shown in figure 3.3. Initially different temperatures were used for the curing process. The optimum temperature for the formation of the channels was found to be within the range of 110- 120°C. The diameter of the channels was in hundreds of micrometers. Confocal photomicrograph of one of the channels formed by this technique is shown in figure 3.4. These channels did not extend from the bottom to the top, rather these channels were found to be closed from both ends. The channel was tapered and there was variation in the channel diameter with a slight constriction at the bottom. These membranes were sliced on both sides to obtain through channels [8].

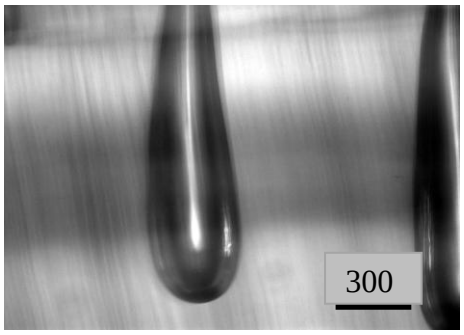

Fig. 3.4 Confocal photomicrograph of a single channel formed with PU beads.

3.3.2. Experimental Methods (Iron-oxide nanoparticles)

Self aligned channel formation in the nanometer scale required the application of 30 nm iron particles. The particles were placed on top of a Petri dish and PDMS was spread on top of these nanoparticles. Polymerization of PDMS was carried out on a hotplate. Alignment of the iron-oxide particles was achieved by applying a magnetic field. The magnet conferred directionality and helped align the nanoparticles. A schematic of the entire process is shown in figure 3.5.

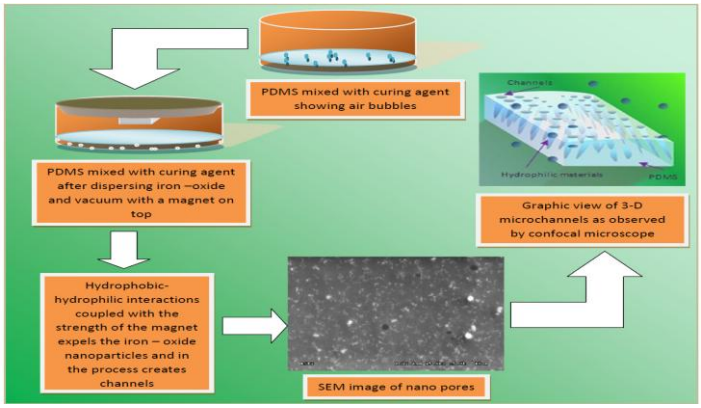

Fig. 3.5 A schematic of the entire process of fabrication

The hydrophilic iron-oxide nanoparticles formed clusters as they were dispersed in the hydrophobic PDMS polymer matrix. The polymerization of PDMS on a hotplate leads to

solidification of the polymer from the bottom to the top. This is known as directional polymerization. As the polymerization ensued, the iron-oxide nanoparticles were pushed through the liquid matrix before polymerization of the pre-polymer in that region occurred. A direct implication of this is that the curing rate is a determining factor on whether the iron-oxide nanoparticles are capable of forming the microfluidic channels by being expelled out or they being entrapped in the polymer matrix. The curing rate of the pre-polymer in turn depends on the amount of curing agent utilized and the temperature at which the curing takes place. The principle behind the formation of channels using iron-oxide nanoparticles is shown graphically in figure 3.6.

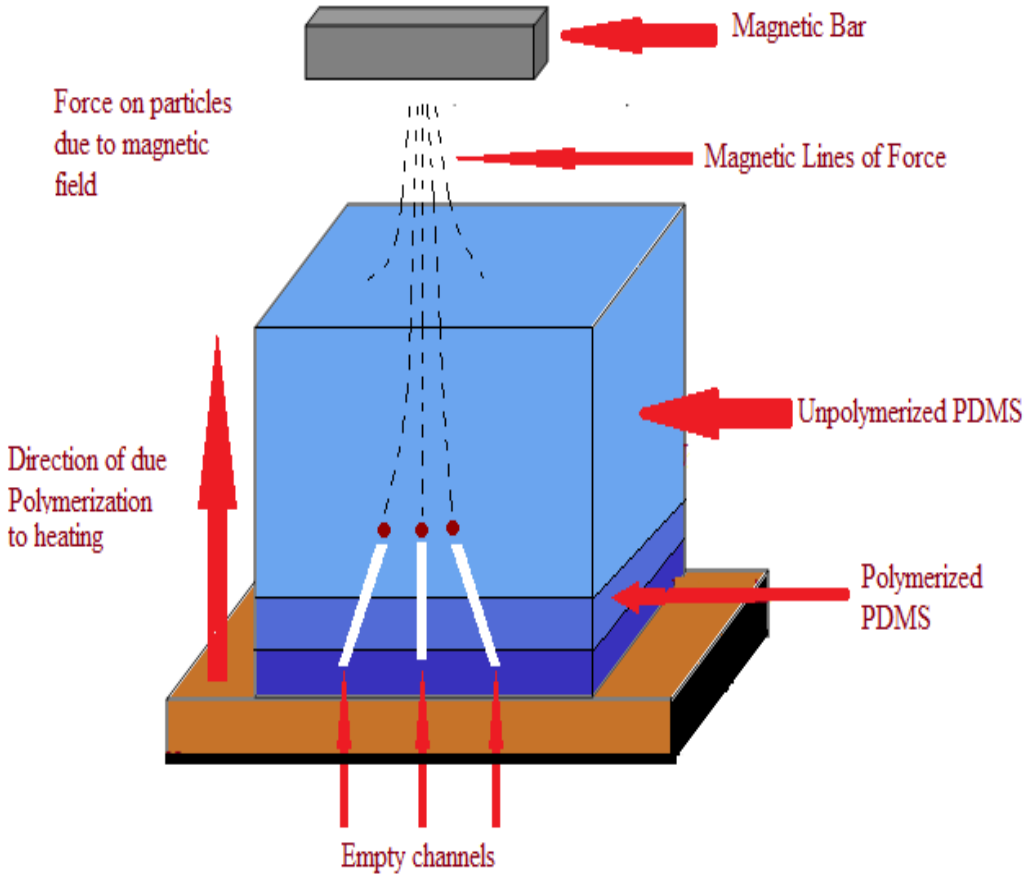

Fig. 3.6 Principle of fabrication of microfluidic channels using iron-oxide nanoparticles

To prove iron-oxide nanoparticles are hydrophilic and to clarify that the magnet was used only to provide directionality and alignment, the above experiment was conducted in the absence of the magnetic field. SEM images in figure 3.7 clearly show that the iron-oxide nanoparticles have been pushed to the surface of the PDMS as it was being cured. This ascertains the fact that hydrophilic moieties are expelled from the hydrophobic polymer matrix, whether exposed to magnetic field or not. However, the force exerted by hydrophobic PDMS was not sufficient to push all the particles upward /out of the PDMS.

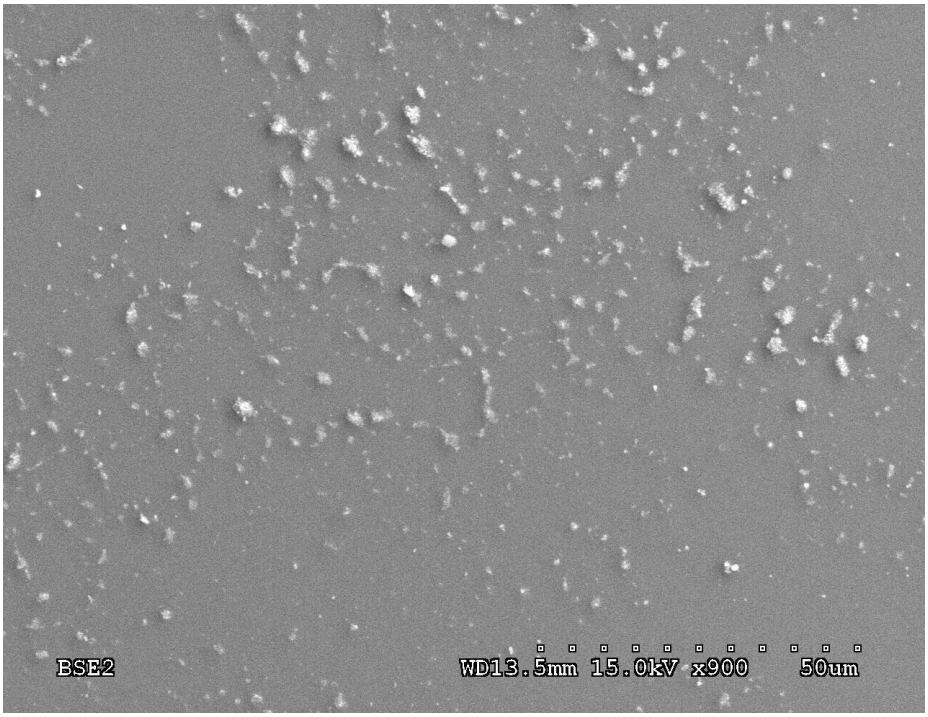

Fig. 3.7 Iron-oxide nanoparticles on the surface of the PDMS without using a magnet for directionality [8]

The rate of polymerization depends on the temperature and as the temperature increased viscosity at the particle-polymer interface increased very fast. This was attributed to the fact that local polymerization at the metal-polymer interface quickens as the metal particles

absorb heat. A direct consequence of this is the entrapment of many particles inside the matrix. This called in for a controlled magnetic field that served two purposes: (1) Pushed the particles against the localized polymerization and (2) Provided directionality and aligned the nanoparticles [8].

The iron-oxide nanoparticles employed in this work were 30 nm in diameter. Hence, the expected outcome was the formation of 30 nm channels, but the dimensions of the channels were in hundreds of nanometers. This was attributed to the fact that the viscosity of liquid PDMS collapsed the chains, forming small agglomerations of particles. The particle clustering can also be attributed to the van der Waals force which is attractive in the nanometer range or the hydrophobic clustering effect discussed in section 3.2.1. SEM micrograph shown in fig. 3.8 illustrates the pores obtained in the nanometer dimensions. The diameters of the pores are around 200-300 nm which are in accordance with the earlier conclusions.

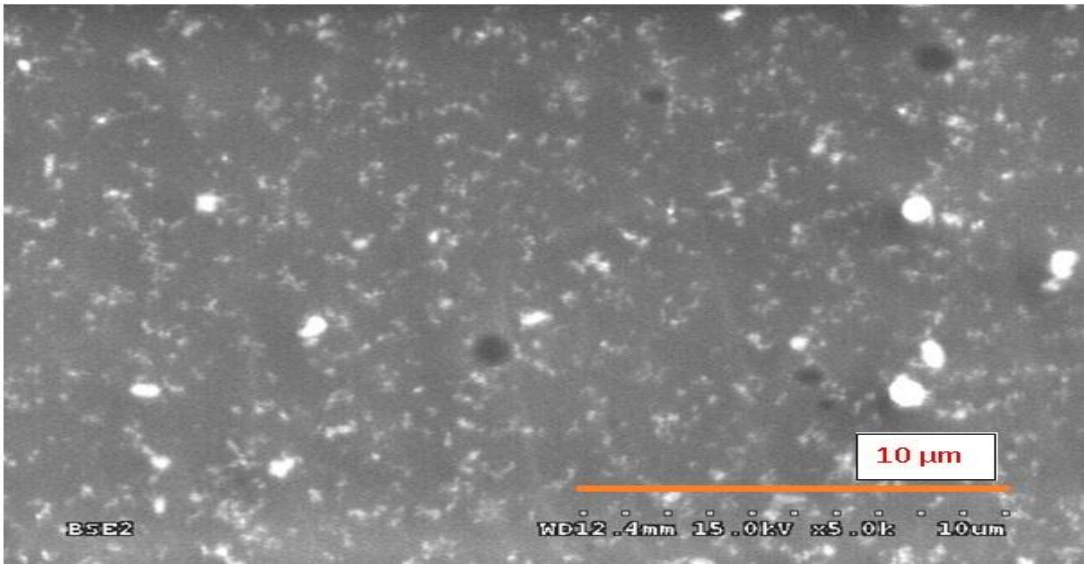

Fig. 3.8 SEM micrograph of microfluidic channels obtained in nanometer dimensions[8]

The work here presents a novel approach to create microfluidic-channels without the

use of lithographic techniques. These bench-top techniques are simple, cost effective and rapid and can be employed in laboratories and research environments were microfluidic channels are required for preliminary analysis. The study explores the possibility to obtain uniform pore sizes with a certain degree of alignment. It is however important to realize that the alignment achieved previously using soft lithography cannot be achieved by the approach presented here at present (for example work of reference [15]). But on the other hand the process can be completed within 30 minutes, provides channels of similar dimensions with little alignment options. The price paid for lowering the cost and time of fabrication is in terms of precision in alignment [8].

3.3.3. I-V measurements in PDMS microchannels

The membranes were subjected to a Current-Voltage characterization based on which their length was characterized.

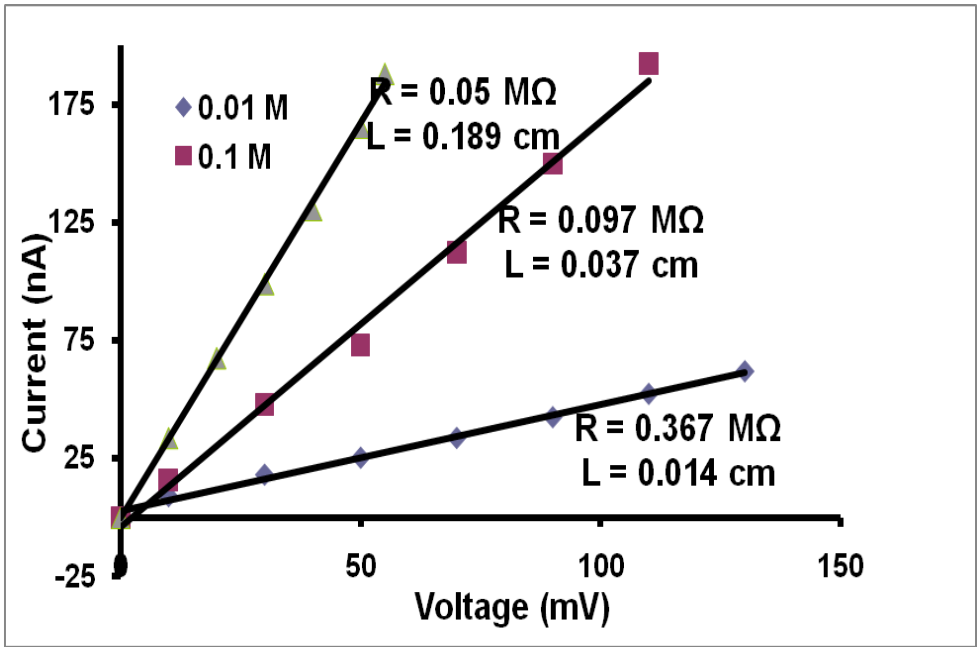

Fig. 3.9 Current- Voltage measurements for different concentrations of KCl through PDMS pores

It was assumed the resistance in all the channels (with the same diameter 300±10µm and length) were identical. Different concentrations of KCl were used and conductivity *(σ)* of the solution was calculated using the formula $\sigma = nq\mu$ where *n* was the number of ions, *q* was the charge of an electron, and *µ* was the mobility of the ions. The resistance *R* was calculated from the *I-V* measurement data shown in figure 3.9.

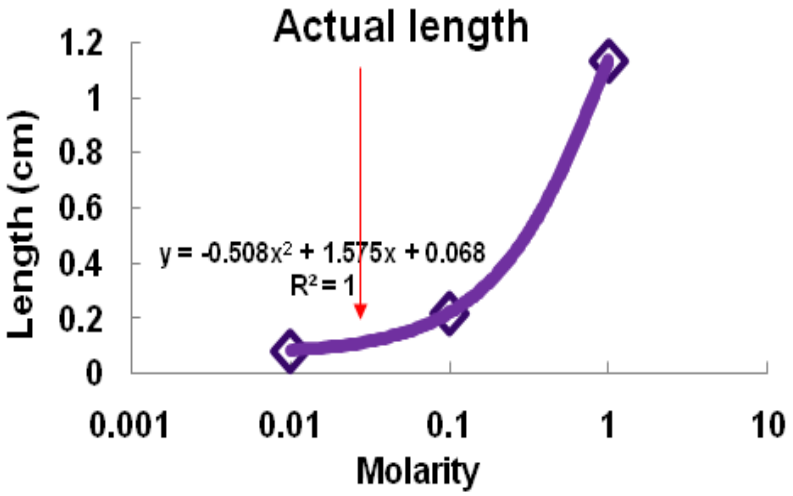

Fig. 3.10 Length Vs Molarity

The length of the channel was calculated using the formula $R = \frac{\rho L}{A}$ where *ρ* is the resistivity, *L* is the length of the channel and *A* is the area of the cross-section of the channel. The variation in calculated length with molarity is shown in figure 3.10.

The variation in length of the channel was attributed to charge build up on the PDMS due to dissociation of the silanol groups. The length of the channel was large for low molarity, and the reason was attributed to the decrease in conductivity due to fewer ionic carriers and increased contribution from the surface charge at low concentrations. This leads to an increase in resistance and hence the increase in the calculated length. Electric field across the channel is

given by $E = \frac{-\varphi}{L}$ where L is the length of the channel and ϕ is the applied bias. The electro-osmotic flow mobility μ_{EO} of the ions through the channels is given by $\mu_{EO} = \frac{V_{EO}}{E}$ where V_{EO} is the flow velocity. Thus it can be seen that $\mu_{EO} \propto -L$, implying that the calculated length of channel is very large when we have very low mobility which was observed at high molarity. The Smoluchowski equation is $\mu_{EO} = \frac{-\zeta\varepsilon}{\eta}$ where ζ is the zeta potential, ε is electrolyte permittivity and η is the dynamic viscosity. The only factor that can influence the mobility when the temperature and molarity are constant is ζ. At higher molarity the lower mobility is hence due to silanol dissociation on PDMS walls increasing ζ [8].

CHAPTER 4

POLY(ETHYLENE OXIDE) (PEO) AS THE HYDROPHILIC MATERIAL FOR MICROFLUIDIC CHANNEL FABRICATION

This section describes the use of the commonly used poly (ethylene oxide) (PEO) as the hydrophilic material in the fabrication of micro/nano channels in polydimethylsiloxane (PDMS) using hydrophobic-hydrophilic interactions. The introduction of PEO for this novel technique of micro/nano channel fabrication provides ease of handling, better inherent alignment and excellent repeatability. One of the remarkably consistent results of the experiments was the tapered structure of the channels obtained. These channels were closed from both the top and the bottom. Thin layers of PDMS membranes were sliced in order to create 'through' channels. It was observed that the slicing of the PDMS provided us with channels whose dimensions can be approximated to be cylindrical. These cylindrical *'through' channels* have been proved to form membranes and preliminary studies indicate that these can be used as micro- reactors for protein purification experiments and we also propose that these channels could potentially be used for *in vitro* simulations for analysis of blood flow through capillaries.

4.1 Materials

In this chapter we compare the different hydrophilic materials that were used for fabrication of microfluidic channels, the difficulties encountered in each of them, the subsequent modifications and the final protocol for fabrication of microfluidic channels.

4.1.1. Iron-oxide Nanoparticles

Iron-oxide nanoparticles obtained from Nanostructured and Amorphous Materials Inc. were used as such. The dimension of the iron-oxide nanoparticles utilized for these experiments

was 30 nm. The final dimension of the channels obtained from these nanoparticles did not reflect the initial dimension of these particles as these were subjected to nanoscale forces which led to the agglomeration of particles. A bar magnet was used for the alignment of these nanoparticles.

4.1.2 Polyurethane beads

Tecoflex polyurethane beads obtained from Lubrizol Incorporation was used as such. The diameters of these beads were of the order of 2- 3 mm. The final dimension of the channels did not reflect the size of the beads as these beads were softened by heat at elevated temperatures around 300 °C before the experiments were performed. This led to channel fabrication in the range of 500 microns [8].

4.1.3 Poly (ethylene oxide) microspheres

Poly (ethylene oxide) microspheres (Avg. MW-200,000) were obtained from Sigma Aldrich corporation and were used as such. The PEO microspheres were heated to 250 °C where they melted instantaneously. The channels formed with PEO were much smaller than those observed with polyurethane beads. The channel dimensions were around 100-250 µm. A comparison between these two is more relevant than that with iron nanoparticles because both PU and PEO microspheres are polymeric materials and before the experiments were begun both these hydrophilic materials were subjected to very high temperatures and melted. On the other hand the forces that iron-oxide nanoparticles were subjected to were clustering, electrostatic and van der Waal's forces at nanoscale.

4.2 Fabrication Protocol

The steps employed in the fabrication of the microchannels using iron-oxide nanoparticles and Tecoflex polyurethane beads have been described in detail in chapter 3. Briefly, PDMS mixed with curing agent in the ratio of 10:1 was degassed for around 30 minutes to 1 hour. In the case of Tecoflex Polyurethane (PU) beads, the polymer was melted at 300 °C. The temperature was then lowered to around 100 °C before the PDMS was poured on top of it

and cured. The channels were formed because the partially molten PU beads were ejected out of the PDMS polymer matrix.

For iron-oxide nanoparticles, a similar technique was followed. The PDMS was mixed with the curing agent as reported above and degassed. The iron-oxide nanoparticles were placed on the bottom of the Petri dish. Care was taken to see that the iron-oxide nanoparticles were evenly distributed when PDMS was poured over. Alignment of nanoparticles was not accurate and this led to the agglomeration of the nanoparticles and the subsequent larger channel dimensions. PDMS was poured on top of the iron-oxide nanoparticles and it was subjected to curing. A magnet was used to provide directionality [8].

The protocol followed for the fabrication of microchannels using poly (ethylene oxide) microspheres has been described in detail below. The physical state of the PEO used in these experiments can be considered to be powder or flakes with an average molecular weight of 200,000.

1. The hydrophilic PEO particles are measured using a weighing scale. 10, 20, 30, 40 mg of particles were measured and taken in an Eppendorf tube.
2. A 30 mm Petri dish was first cleaned with ethanol and acetone. (Note: The Petri dish has to be clean to prevent the PEO particles from being contaminated and to keep these dry to ensure that they do not stick to the Petri dish).
3. The measured PEO particles were placed in the Petri dish. They were aligned in such a way that all the PEO particles were accumulated at one point. A schematic is shown in fig. 4.7.
4. In another formulation, the PEO particles were weighed and dispersed on the Petri dish. The distribution of the PEO on the Petri dish was not controlled
5. PDMS was mixed with the curing agent in the ratio of 10:1 in a 50 ml beaker.
6. PDMS was then degassed inside a vacuum chamber for 30 minutes to 1 hour. Initially the surface of PDMS was clear without any ripples when it was placed

inside the vacuum chamber. Ripples and air bubbles were observed after approximately 5 minutes inside the vacuum chamber. The PDMS was placed inside the vacuum chamber till no air bubbles were observed during inspection.

7. The PEO particles placed on the Petri dish were moved to a hot plate which was at 250 °C. It was observed that the PEO particles lost their powdery microsphere structure and transformed to a viscous molten state under the influence of the temperature.
8. **CRITICAL STEP-** The PDMS was poured on top of the viscous PEO. The PDMS had to be carefully poured exactly on top of the molten PEO for the formation of channels when step 3 was followed. On the other hand, the manner of PDMS dispersal on the Petri dish was not crucial when performing the formulation of step 4.

4.3 Results

Poly (ethylene oxide) is also referred to as poly ethylene glycol. It is a synthetic polymer that is soluble in water and a few other organic solvents [58]. It is biocompatible and has been studied extensively for its reportedly low toxicity [59, 60]. Because of its ability to dissolve in both water and other organic solvents it is sometimes called and an amphiphilic polymer. It often forms the hydrophilic end of the amphiphilic polymer micelles that are fabricated for various purposes. The hydrophilic nature of PEO is exploited when it is used for the purposes of preventing non- specific adsorption of proteins and cells [61]. The PDMS structure has n[–Si(CH3)$_2$–o–]n [62]. This makes it inherently hydrophobic [63]. The silicone chains are highly flexible and hence they can rearrange to form hydrophilic silanol groups when in contact with water or when it is subjected to oxygen plasma. But the high flexibility of the low molecular weight siloxane chains in the bulk of the PDMS allows it to permeate to the surface restoring its hydrophobicity very easily [63, 64]. There have been previous studies on the interactions between PEO and PDMS to created PEO tethered PDMS substrates to prevent

protein adsorption [65, 66]. PEO tethered PDMS surfaces were fabricated by dipping small pieces of PDMS in a solution containing the block co-polymer of PDMS and PEO.[67]. To the best of our knowledge, interactions between PEO and uncured PDMS have not been reported elsewhere. Previously in Sankaran et al. (2011) [8], we reported similar interactions between hydrophilic materials and hydrophobic polymer matrix. The hydrophilic materials employed there consisted of iron-oxide nanoparticles and polyurethane beads.

The iron-oxide nanoparticles used previously were 30 nm in diameter and were difficult to handle in terms of alignment, controllability and repeatability.

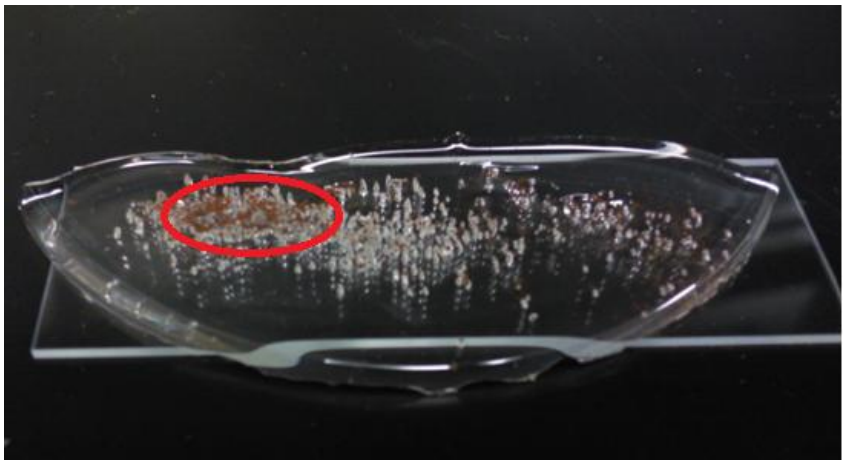

Fig. 4.1 Iron nanoparticles (brown) shown in the circled area have collapsed under the viscosity of PDMS and the strength of van der Waals forces

The metal-oxide particles were a very fine powder and were magnetic. These thus had very strong van der Waal's interactive forces. Experimentally, it was observed that these forces at the nanoscale were attractive. This led to the agglomeration of these nanoparticles as shown in fig. 4.1 above.

Alignment of clusters of such nanoparticles was achieved by the application of a magnetic field as shown in fig.4.2.

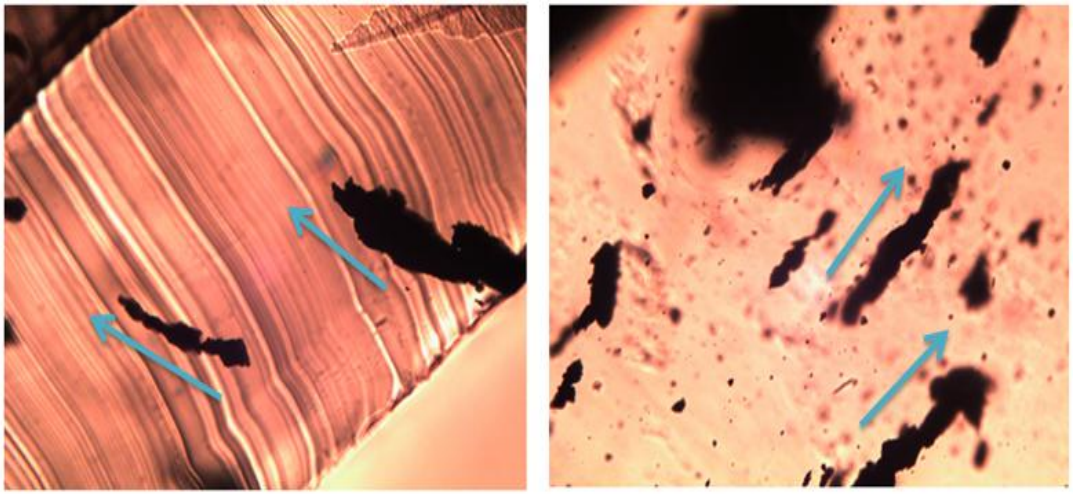

Fig. 4.2 Alignment of iron nanoparticles towards the top surface where the magnet was placed (left)
Alignment of nanoparticles as observed from the top view (right)

However there was no control over the size of the clusters formed and hence the dimensions of the channels. Moreover the length of such channels did not extend all the way to the top surface of the PDMS membrane (illustrated in fig. 4.3).

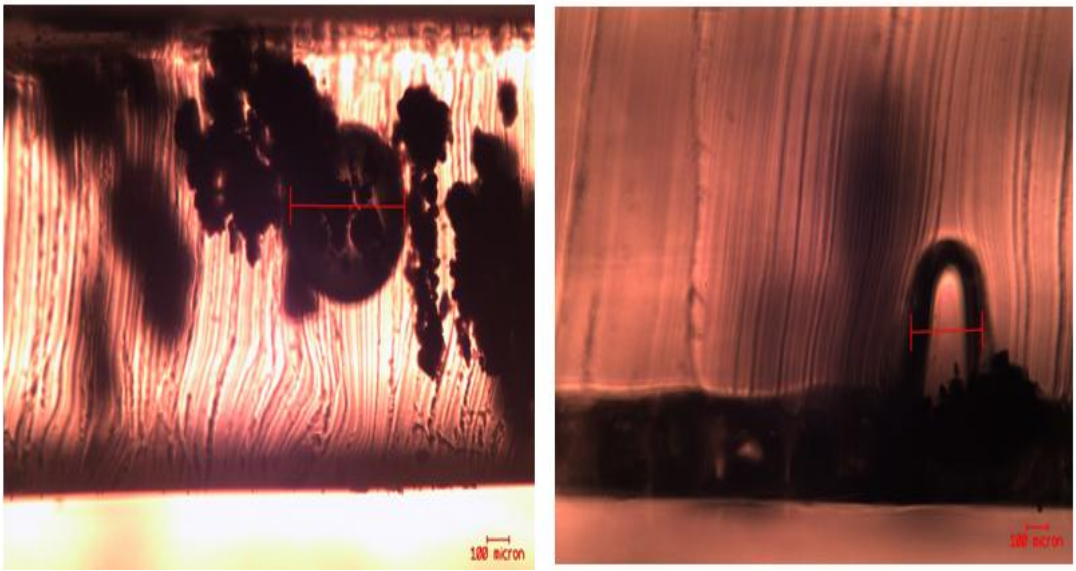

Fig. 4.3 Optical micrograph of iron nanoparticles agglomerating forming collapsed chains under the viscous forces inside PDMS (left). The channels formed are very small in length extending only to very minute distances from the base (right).

Possible explanations to this phenomenon could be that the strength of the van der Waals forces was much higher than the energy provided by the change in entropy [8, 68]. Moreover as the nanoparticles moved along the direction of polymerization and hence the increase in viscosity of the surrounding polymer matrix exerted frictional forces which could have reduced the mobility of the iron-oxide nanoparticles. A relation between temperature and porosity and pore size was not detailed for formation of channels before. It was observed that temperature did not have a direct impact on the size of the channels formed. The dimensions of the channels were limited by the extent of clustering of the iron-oxide nanoparticles. Moreover it was observed that an increase in temperature did not favor porosity. This could be attributed to the fact that an increasing temperature would result in rapid curing rate. The energy released by the change in entropy [69] was not sufficient to counter the combined forces of van der Waals interactions and viscosity acting in the opposite direction. This called for a controlled curing rate. The controlled curing rate was achieved by maintaining a low temperature of around 80 °C for curing for prolonged durations. Optical micrographs showed the length of the channels formed at lower curing temperature (Fig. 4.4).

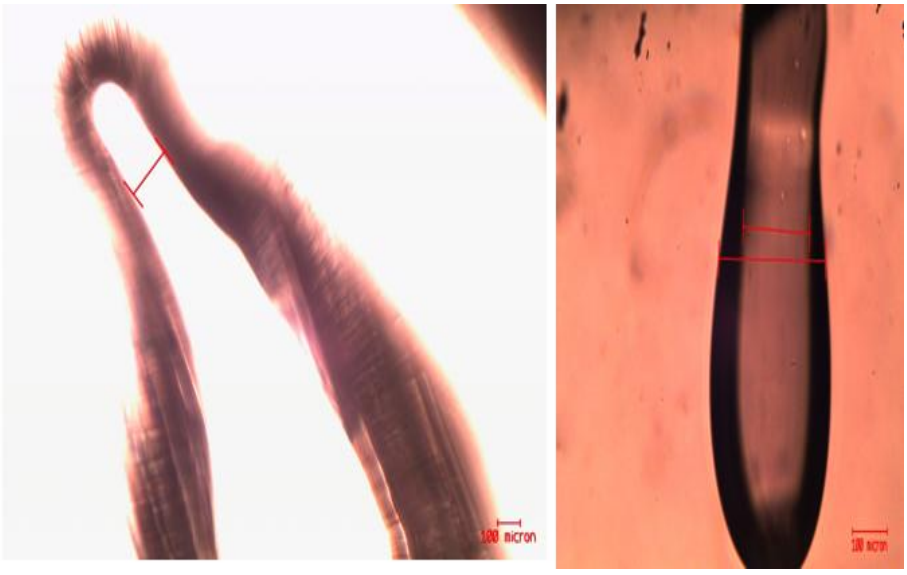

Fig. 4.4 Optical micrographs of microfluidic channels formed using iron-oxide nanoparticles at 80 °C

Another material reported in Sankaran et al [8], for the fabrication of channels was the hydrophilic Lubrizol tecoflex polyurethane beads. We reported experiments at a temperature range between 112-120 °C. It was found that the channels obtained were produced by the vapors of polyurethane beads rather than the polymer rising through the PDMS matrix. The tecoflex beads stuck to the bottom of the Petri dish when such experiments were conducted. If the PDMS membrane was removed from the Petri dish after curing, it was found that the hydrophilic beads were embedded in the polymer matrix. Studies were conducted to liquefy the beads by heat before curing as shown in figure. 4.5 (top left). The experiments were conducted at different temperatures. It was found that the beads had a very high glass transition temperature. It is the temperature at which the state of a polymer changes from a glass like brittle state to a more viscous rubbery state (illustrated in fig. 4.5 top right). At such high temperatures it was found that the PU beads underwent discoloration and the PDMS matrix cured instantly. It was found that at these temperatures, the PDMS stuck to the Petri dish and the membrane suffered mechanical damage when it was removed from the dish.

Microfluidic channels with diameter in the range of 300-500 µm was obtained with PU beads. The channels were uniform and there was inherent alignment because the beads could be aligned manually. The channels were closed from both ends. The difficulties faced were in terms of ease of fabrication, removal of membrane without mechanical damage and critical control of the high temperature.

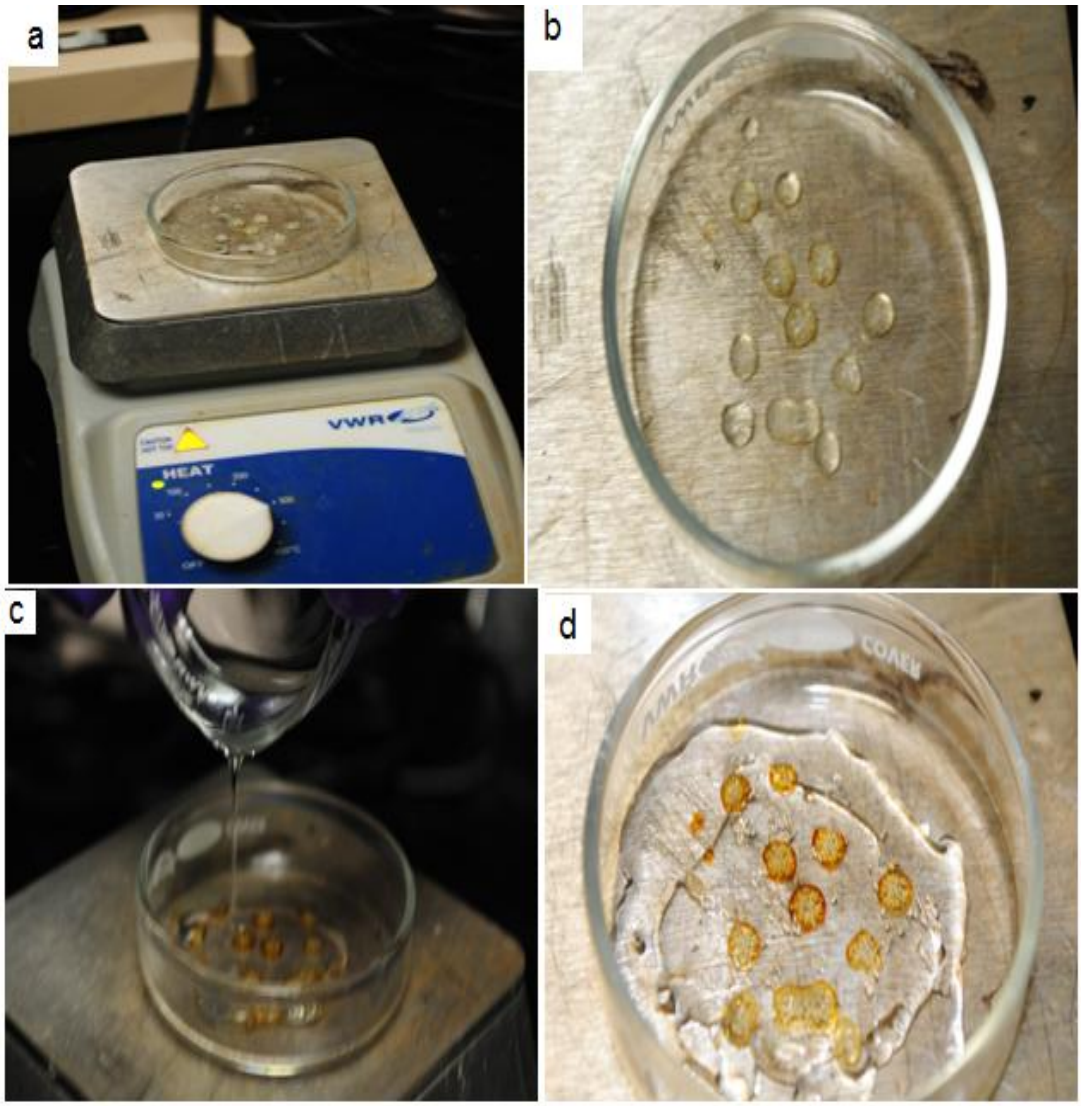

Fig.4. 5 The temperature was raised to 300 °C to produce a phase change in the PU beads (top left).The beads liquefied and the droplets clustered at high temperatures (top right). As the temperature was maintained the PU beads changed color (bottom left) and PDMS was poured on top of it for instant curing. Microfluidic channels could still be seen around the molten PU beads (bottom right).

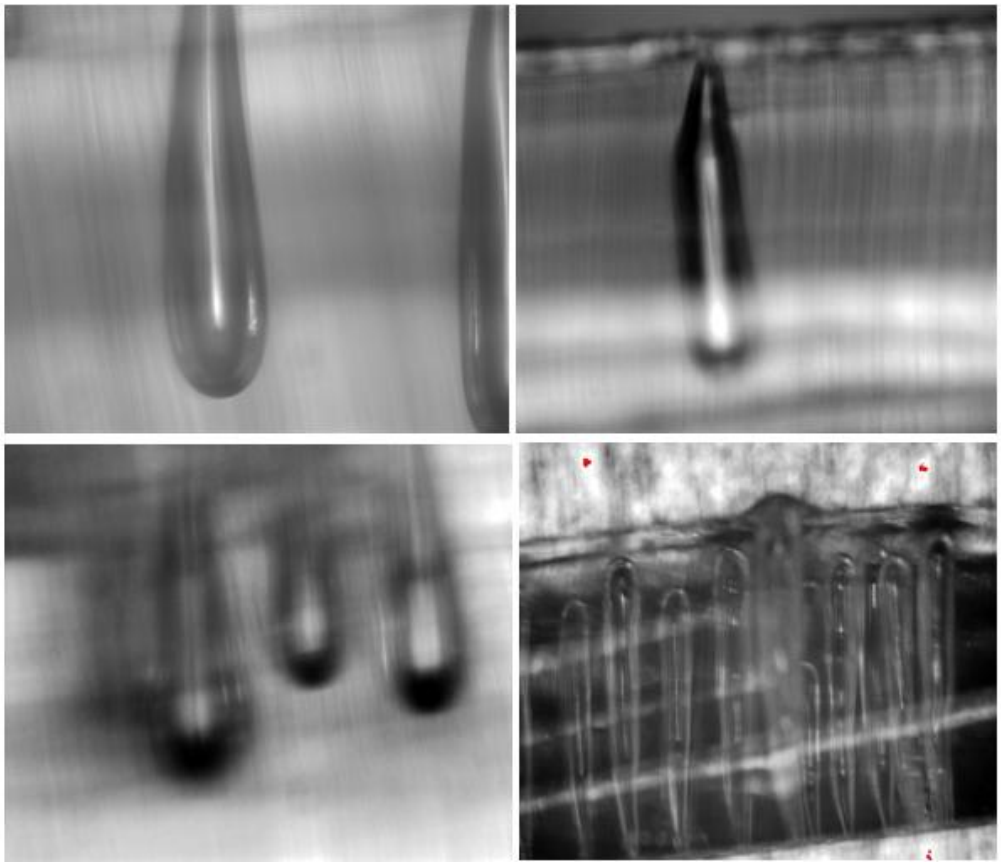

Fig. 4.6 Confocal micrographs of microfluidic channels formed using PU beads on PDMS (top). The channel diameter and distribution is uniform (bottom). The length of the channels varied throughout the membrane. As the temperature was increased drastically, the length of the channels increased to extend to the entire thickness of the PDMS

The quest for a new hydrophilic material was launched in an effort to combat the issues associated with the fabrication of microfluidic channels based on iron-oxide or PU beads. The new material had to satisfy certain primary requirements. The material had to be a polymer, so that it did not store heat as the temperature for curing was at an elevated range. It should preferentially not aggregate, and has a low liquefaction temperature. It should not intercalate with PDMS. The PDMS should not react with the polymer. The polymer should not be a solvent or swelling agent of PDMS. It should have the ability to withstand a range of temperatures (specifically the range within which PDMS is stable) and preferably, it should be biocompatible.

This led us to use PEO which met most of the stringent requirements posed by this work. The fabrication of channels using PEO is detailed in the section above.

A few interesting aspects were observed when microfluidic channels were fabricated with the help of PEO microspheres. The relation between the amount of PEO employed and the porosity was obtained by employing different quantities of PEO accumulated at one particular spot as shown in fig.4.7.

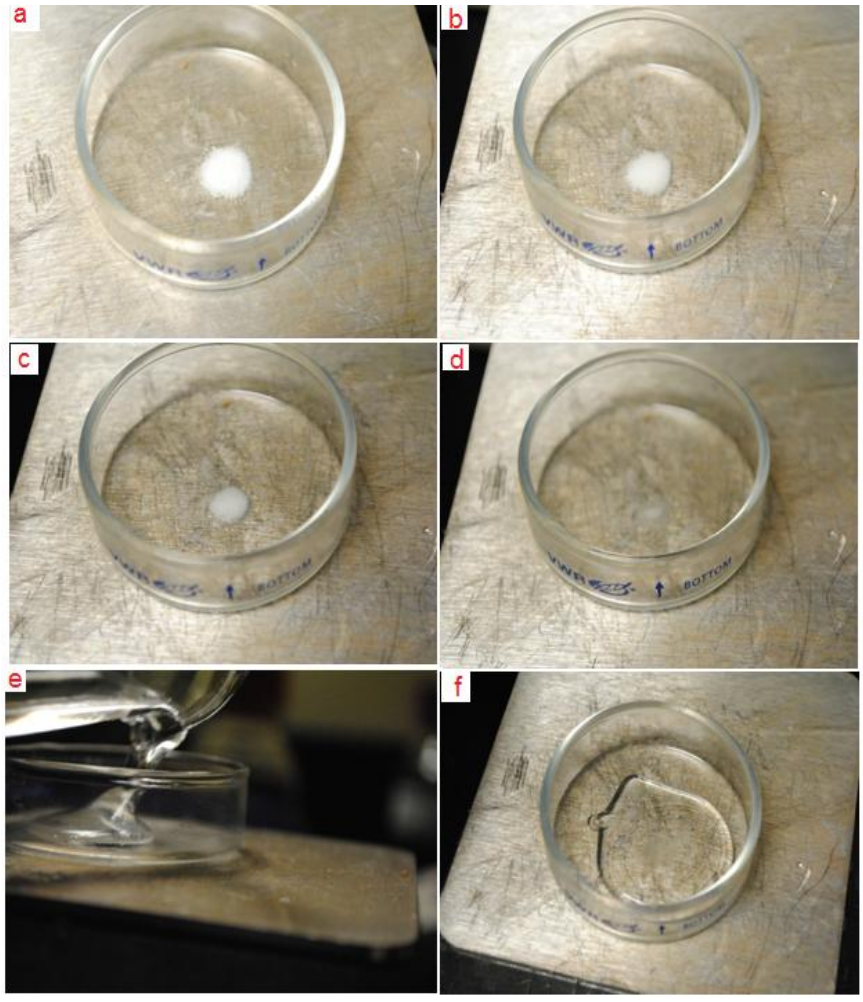

Fig. 4.7 (a), Measured quantity of PEO is taken in an Eppendorf tube and inverted over one particular spot on the Petri dish placed over a hotplate, (b, c, d) The PEO particles under the influence of heat at different time points, (e) PDMS poured over the molten PEO, (f) The PDMS curing and channel formation as PDMS cures.

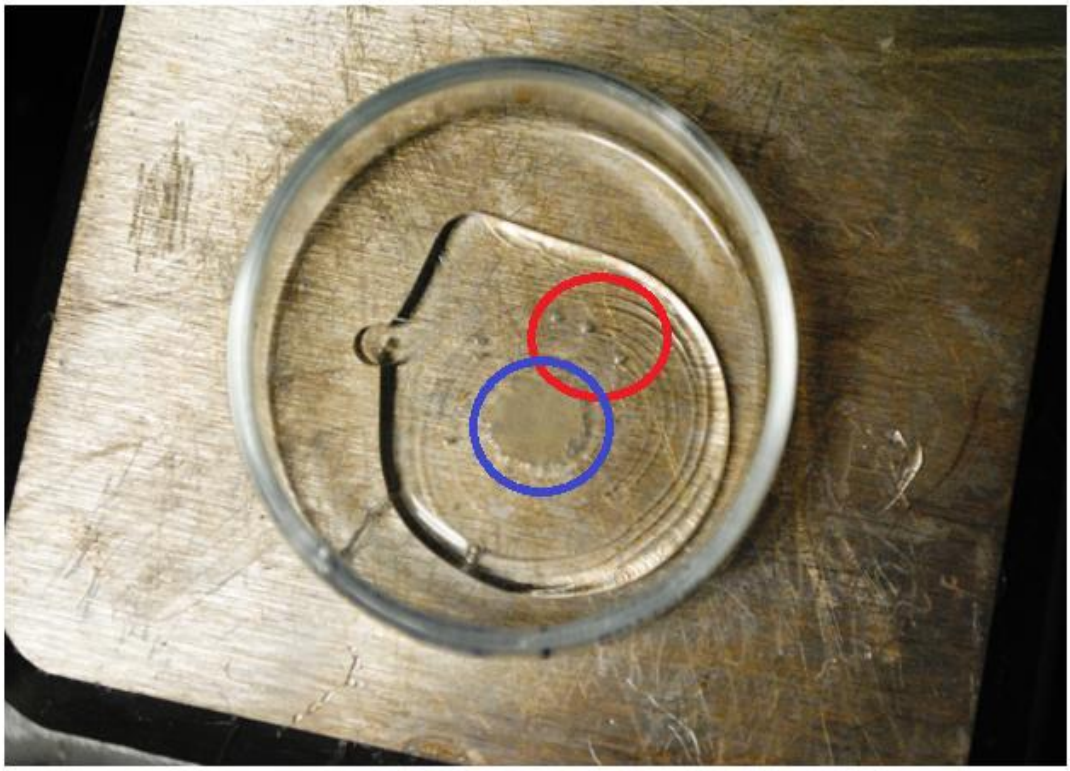

Fig. 4.8 An enlarged image of fig. 7(f) illustrating the formation of channels as the PDMS cures (red) and the location where PEO was dispersed (blue)

Different quantities, specifically, 10, 20, 40 and 50 mg were used to conduct these experiments. These quantities of PEO were separately employed in the Petri dish as shown in fig. 4.7. It was observed that no channels were observed in the area where PEO was actually placed on the Petri dish as shown in fig. 4.8. The interactions between the molten PEO were strong and hence the force exerted by the PDMS, resulting from the enthalpy produced from the polymerization reaction was not sufficient. It can be seen from fig. 9 that the channel formation further depended on the PEO particles that were dispersed on the periphery of the actual bulk mass at the center. One of the interesting physical phenomena was the horizontal oscillatory bulk motion of the PEO inside the polymer matrix during the formation of microfluidic channels. The forces that bind the PEO particles amongst themselves include the van der Waals forces at the nanoscale [70], the viscous force also tends to collapse the PEO particles at one place, and

moreover the liquefaction of PEO particles could result in interaction between the molecules of adjacent PEO microparticles under the influence of heat to crosslink among themselves. The properties of PEO have often been a vastly debated topic mainly because of its unusual hydrophilic character. Both poly butylene oxide and poly methylene oxide are hydrophobic which is often attributed to their pendant methyl groups. It has also been reported that PEO in water undergoes hydrophobic interaction which is essentially entropic in nature, i.e. attraction between aggregates increases with increasing temperature. Through this work we propose that PEO undergoes similar interaction with PDMS, but it is coupled with the van der Waals attractive force which leads to their aggregation at high temperatures [70, 71]. Furthermore, there are earlier studies indicating that PEO interactions are repulsive at long range while attractive at short ranges [70].

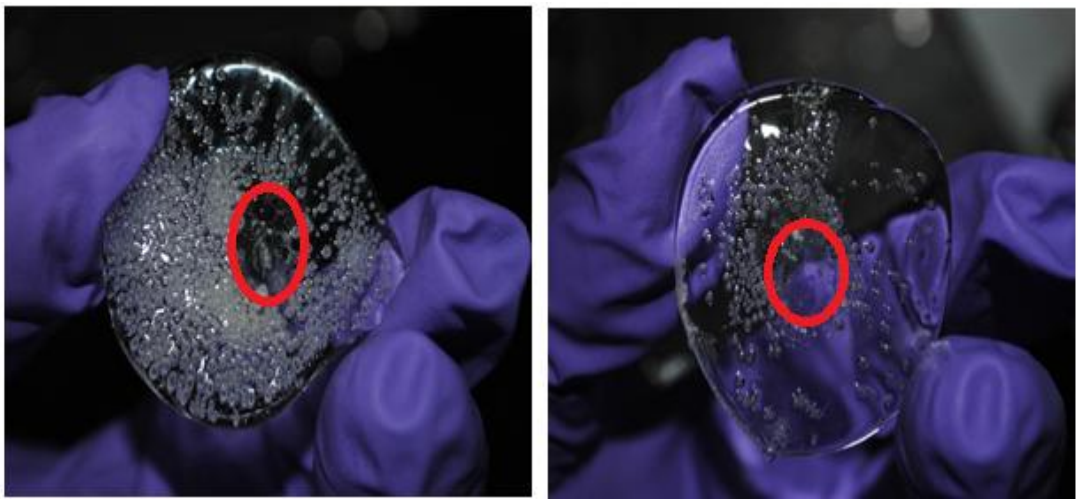

Fig.4.9 10 mg of PEO accumulated inside the red circle (left) with dispersed PEO on the side. It was seen that the PEO in the bulk moved horizontally as described in the above section. Moreover it was observed that the PEO at the periphery in such groups tried to break away from the bulk. These PEO droplets that break away produce channels as shown in the figure along with the other PEO particles lightly dispersed over the entire area. 40 mg of PEO was used in the right. It can be observed from these images that as the PEO are accumulated in one area, the tendency for channel formation decreases. A dispersed alignment is required for optimal control.

The complex interplay between attractive and repulsive forces has not been completely understood. But, it could well be the reason for the horizontal kinetic energy that makes the molten PEO chains thermally oscillate within the PDMS matrix. The introduction of the term thermal oscillation in this context is apt because the motion of PEO was observed even after the PDMS matrix was removed from the hot plate. Even after curing, the thermal vibrations continue and cease only when the temperature of the matrix falls considerably and the physical and chemical crosslinking within the PDMS matrix becomes strong enough to offer very high viscosity. The reason why these interactions between PEO amongst themselves and PEO with PDMS and PEO with water are important is because these allow us to understand the physics underlying polymer-polymer reactions. It can be extended to polymer-bio-polymer interactions like PEO-protein, PDMS-protein, PEO-PDMS-protein interactions because the forces at the nanoscale that define these interaction could well be uncovered by understanding these fundamental process that we observed during this work. Principles and theories relating to PEO-water interaction have been extensively studied and several useful correlations have been figured.

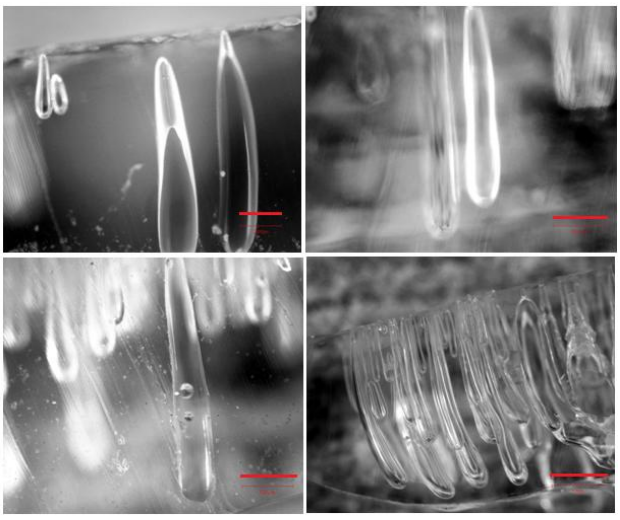

Fig. 4.10 Confocal photomicrographs of PEO microfluidic channels at 250 °C (top left), 275 °C (top right), 300 °C (bottom left), and 325 °C (bottom right). The scale bar is 200 micron for the micrograph at 250 °C while it is 500 micron for the images at 275 °C and 300 °C. The scale bar is 1 mm for the 325 °C sample of PDMS

When PEO was well dispersed and the lengths of the channels were measured for different temperatures, the length of the channels seemed to increase with temperature. The thickness of the PDMS used was not controlled for this characterization. The temperature of curing was varied between 225 to 300 °C. The channels were found to extend from the base towards the surface. In cases where the PDMS membranes were thin the channels sometimes went all the way to the top surface. The length of the channel seemed to be a function of the temperature and the van der Waals forces between the adjacent PEO microspheres. Since the viscous drag and the rate of polymerization are dependent only on the temperature and not on the thickness of the PDMS membrane, we do not expect the length of the channels to be influenced by the thickness of the PDMS.

The diameter of the channels did not depend on the temperature of curing or thickness of PDMS. The diameters of the channels were dependent on the extent of dispersion of the channels. A huge difference in diameters was not observed for channels formed from 10 mg or 40 mg of PEO accumulated at one place. At this distribution rate there was saturation and the channel diameters were more or less uniform. Small dimension microfluidic channels were obtained when only a few microparticles were dispersed outside the PEO bulk that was accumulated in the center.

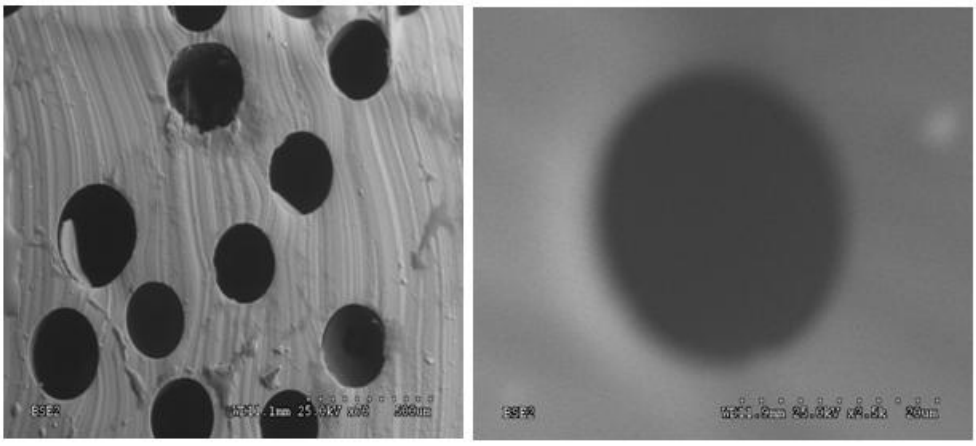

Fig. 4.11 SEM photomicrograph on left shows microfluidic channels , The right micrograph shows zoomed in view of a single microfluidic channel which is around 20 µm in diameter.

The channel dimensions were typically in the range of 250 to 500 µm. Most of the channels were in the range of 300 µm. These images were obtained using the SEM. Most of these channels have a very circular cross section as it can be observed from the images. The shapes of the microchannels are however tapered. The slicing of the microchannels from both the sides resulted in shape of channels to be approximately cylindrical. The potential applications of such microfluidic channels are detailed in the next chapter.

CHAPTER 5

FUTURE WORK

5.1 Protein Purification

The microfluidic channels fabricated using non-lithographic techniques can potentially be used as micro-reactors for protein purification experiments. Proteins are polymers of amino acids and contribute to the mass of an organism to a great extent. A few proteins are abundant in the organisms but a few are very sparse; the complexity of purification increases with the decrease in the ease of obtaining the protein. There are series of steps involved in the purification of proteins. The first is the selection of the source. Then, the proteins have to be solubilized and isolated and then they are purified. There are several methods for the enrichment of proteins; but the most prevalent of these techniques are the chromatographic methods. They are purified based on fractionation procedures. These chromatographic techniques employ a mobile and a stationary phase. The material that needs to be purified is generally dissolved in a solvent and is usually called the mobile phase. It interacts with the stationary phase present in a column. The stationary phase is generally a resin or beads that adsorb the material of interest. Sometimes, the extract might have proteins that have an affinity to the stationary phase based on charge of the stationary phase or chemical affinity to the stationary phase [72-75].

These chromatographic techniques employ a column. In affinity chromatography technique, a thick bed of resin (beads) is formed to ensure that the protein of interest interacts with the resin. The length and diameter of such columns are in macro dimensions while the resin beads are in micro dimensions, which imply the potential surface area for contact is small.

We propose that the microfluidic channels can be used as micro-reactors for enhancing the protein-resin interaction rate and ultimately the purity. By decreasing the dimensions of interaction the total available surface area for interaction can be increased significantly. It is known that the time taken for reactions in microfluidic networks is significantly smaller [76, 77]. It is one of the major advantages of microfluidic systems in the study of chemical reactions.

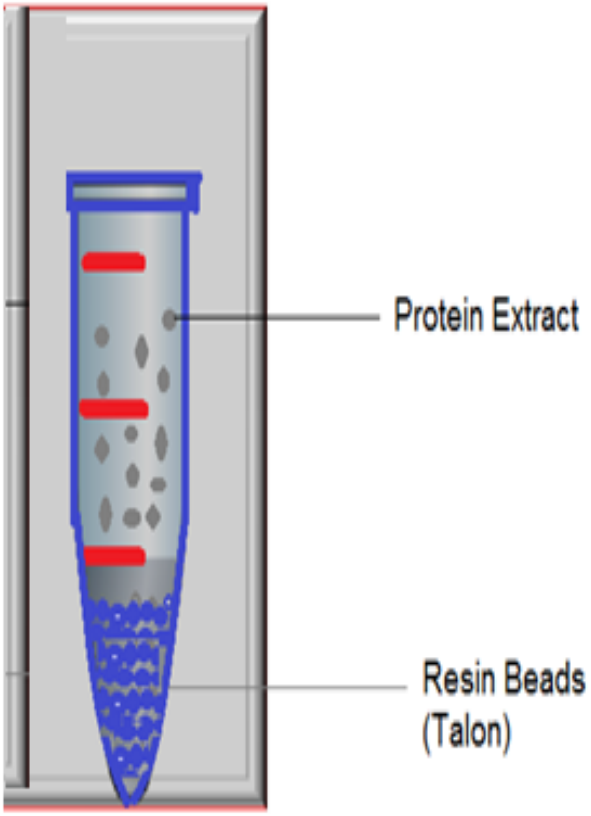

Fig. 5.1 Traditional techniques showing a column filled with the resin and the protein extract

In purification of proteins, the pH, salt concentration, the resin, and the extract composition collectively determine the efficiency of the enrichment technique. It is essential to build a system that conforms to all these factors but should be conceptually efficient. During the lysing of cells to obtain the proteins, detergents are used. Sodium Dodecyl Sulfate (SDS) is a

common detergent used during these techniques. As an initial study the ability of the PDMS membrane to pass different percentage solutions of SDS was tested.

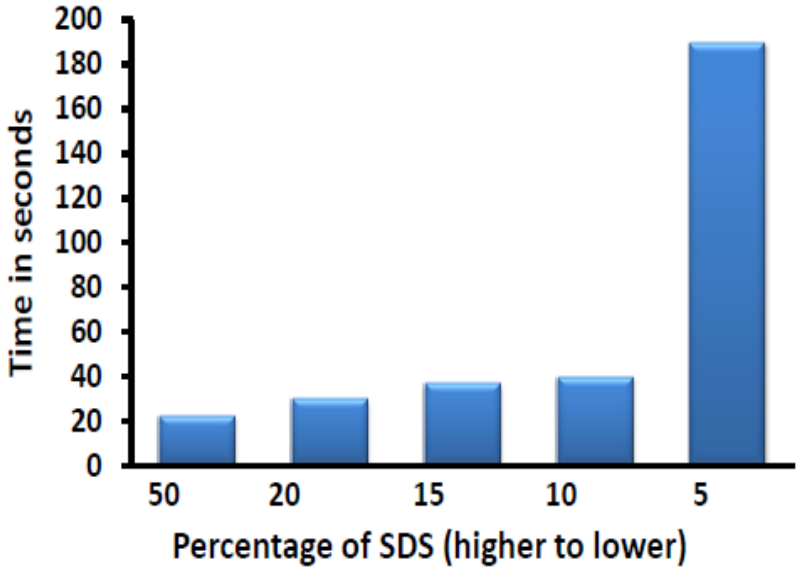

Fig. 5.2 Time vs. SDS percentage solutions. 200 µl of SDS was used in these studies though a slab of PDMS which had an array of microfluidic channels with diameters between 200-400 µm

It was observed that an unmodified surface of PDMS allowed different percentage of SDS solutions at different rates (figure 5.2). As the amount of SDS in the solution increased, the time taken for the solution to pass through the microfluidic channels decreased. Moreover, the amount of SDS recovered also increased with increasing the amount of SDS in solution. The flow of fluid through microfluidic channels in this scenario is by the difference in capillary pressure. The SDS is known to adsorb on unmodified PDMS surfaces. Hence, if PDMS microfluidic channels are treated with oxygen plasma and then subsequently used for protein purification process, they will behave as micro-reactors and will potentially minimize the consumption of the chemicals and enhance the rate of purification.

On a different note, the detergent molecules apparently form micelles. The interaction of these micelles over the microfluidic channel would present another interesting study that

describes the interaction between amphiphilic solvents on a hydrophobic surface. It was found that the rate and the amount of SDS permeating through the PDMS channels varied with the percentage of SDS solution used. The impact of the length and the number of channels under observation has to be analyzed. A thorough study of these aspects along with the velocity profile of the solvent through the microfluidic channel would illuminate us and provide a better understanding of fluid slip at the interface of an amphiphilic solvent and a hydrophobic surface.

5.2 Endothelial Cell Culture

Microvascular networks perform some vital functions like transport of nutrients, oxygen, water and solutes to healthy tissues while removing waste from them [78]. Angiogenesis refers to the formation of new vasculature from the already existing one. Angiogenesis and microcirculation are crucial in the growth and development of tumor cells. They perform similar transport functions but now are also associated with cancer cell metastasis. The tumor vasculature is very different which allows for detection and treatment [79]. The properties of these microvessels namely the hydrodynamic resistance depends on their size, arrangement, number of microvessels, suspended elements in the blood, apparent viscosity of the blood and so on. The blood flow rate in the microvessels can be given by

$$\frac{\Delta P}{FR} \tag{5.1}$$

Where ΔP is the pressure difference between the arterial and venous sides and FR is a complex value that takes into account all possible resistance factors for a system. Blood flow inside microvessels is crucial for any cell in the capillary. Variations in blood flow could have a profound impact on the cells in the circulatory system. Drastic drop in blood flow level can be fatal to the cell. It has also been reported that blood flow is chaotic and the Fahraeus-Lindvist effect is important for oscillatory flow in channels. It would be very difficult to control all these

parameters while working in vivo. On the other hand this system could be tuned down for experiments in vitro for simplicity [79].

Since the inception of microfluidic channels, these experiments are being carried out in vitro but under one major constraint. They are generally carried out on rectangular channels [80-83]. The geometry of the model varies significantly from the circular channels found in nature. These modify the flow rate in the blood vessel, the shear experienced by the cells vary considerably [81].

Endothelial cell culture has been done in PDMS microchannels before for tissue engineering application but it faced a major drawback because they were rectangular in cross section. Studies made on coagulation properties of blood have shown strong dependence on the geometry of the blood vessel [84]. It is vital that work in these areas have to be conducted in circular or cylindrical microchannels like those shown in figures 5.3 and 5.4. We have demonstrated the fabrication of tapered microchannels which can be sliced open to form through channels. The channel dimensions are approximately cylindrical. Complex microfluidic networks have not yet been explored with the new technique of fabrication.

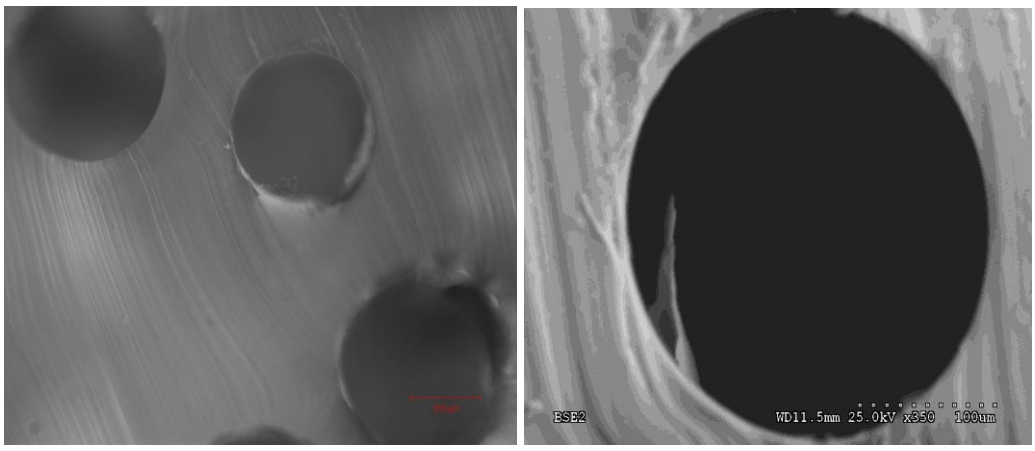

Fig. 5.3 Confocal image of PDMS microchannels (left) SEM image of a single channel (right) The channel dimensions are in the range of 250- 300 µm

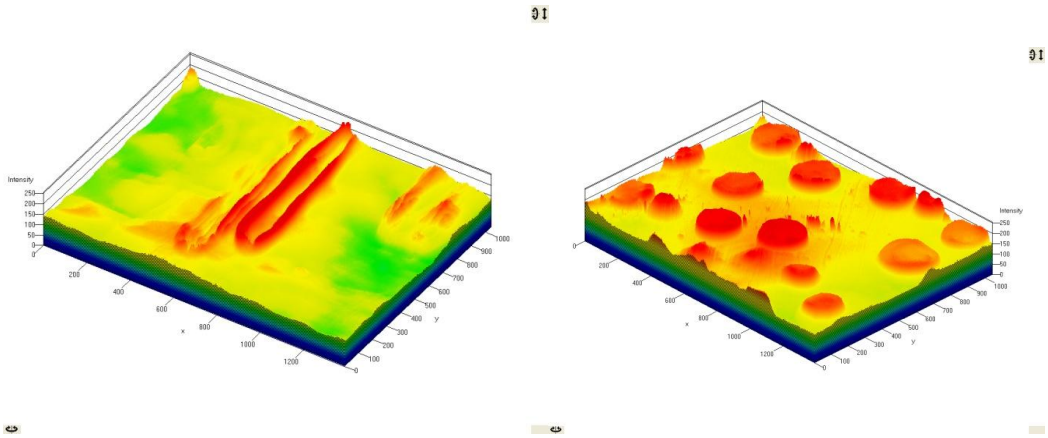

Fig. 5.4 Confocal image showing channels embedded inside the PDMS matrix making it a 3D construct suitable for tissue engineering scaffold applications.

Endothelial cell culture and viability experiments would indicate the ability of the microchannels to act as 3D constructs for tissue engineering applications.

REFERENCES

1. Beebe, D.J., G.A. Mensing, and G.M. Walker, *Physics and applications of microfluidics in biology.* Annual review of biomedical engineering, 2002. **4**(1): p. 261-286.
2. Sia, S.K. and G.M. Whitesides, *Microfluidic devices fabricated in poly (dimethylsiloxane) for biological studies.* Electrophoresis, 2003. **24**(21): p. 3563-3576.
3. McDonald, J.C. and G.M. Whitesides, *Poly (dimethylsiloxane) as a material for fabricating microfluidic devices.* Accounts of chemical research, 2002. **35**(7): p. 491-499.
4. Lee, J.N., C. Park, and G.M. Whitesides, *Solvent compatibility of poly (dimethylsiloxane)-based microfluidic devices.* Analytical Chemistry, 2003. **75**(23): p. 6544-6554.
5. Duffy, D.C., et al., *Rapid prototyping of microfluidic systems in poly (dimethylsiloxane).* Analytical Chemistry, 1998. **70**(23): p. 4974-4984.
6. Xia, Y. and G.M. Whitesides, *Soft lithography.* Annual review of materials science, 1998. **28**(1): p. 153-184.
7. Michel, B., et al., *Printing meets lithography: soft approaches to high-resolution patterning.* IBM Journal of Research and Development, 2001. **45**(5): p. 697-719.
8. Jeyantt S. Sankaran, S.G., Wintana T. Kahsai, Uyen H. T. Pham, Samir M. Iqbal, *Self-Assembled Hydrophilic Interfacing for Thermal Micro Assembly of Polymers (HITMAP).* Advanced Science Letters, 2011. **4**: p. 1-6.
9. Quina, F.H., et al., *Growth of sodium dodecyl sulfate micelles with detergent concentration.* The Journal of Physical Chemistry, 1995. **99**(46): p. 17028-17031.
10. Bruce, C.D., et al., *Molecular dynamics simulation of sodium dodecyl sulfate micelle in water: micellar structural characteristics and counterion distribution.* The Journal of Physical Chemistry B, 2002. **106**(15): p. 3788-3793.
11. Staples, E., et al., *Organization of polymer-surfactant mixtures at the air-water interface: sodium dodecyl sulfate and poly (dimethyldiallylammonium chloride).* Langmuir, 2002. **18**(13): p. 5147-5153.
12. Bordier, C., *Phase separation of integral membrane proteins in Triton X-114 solution.* Journal of Biological Chemistry, 1981. **256**(4): p. 1604.
13. Whitesides, G.M., *The origins and the future of microfluidics.* Nature, 2006. **442**(7101): p. 368-373.
14. Heckele, M., A.E. Guber, and R. Truckenmüller, *Replication and bonding techniques for integrated microfluidic systems.* Microsystem technologies, 2006. **12**(10): p. 1031-1035.
15. Paegel, B.M., R.G. Blazej, and R.A. Mathies, *Microfluidic devices for DNA sequencing: sample preparation and electrophoretic analysis.* Current opinion in biotechnology, 2003. **14**(1): p. 42-50.
16. Khandurina, J. and A. Guttman, *Bioanalysis in microfluidic devices.* Journal of Chromatography A, 2002. **943**(2): p. 159-183.
17. Woolley, A.T. and R.A. Mathies, *Ultra-High-Speed DNA Sequencing Using Capillary Electrophoresis Chips.* Analytical Chemistry, 1995. **67**(20): p. 3676-3680.
18. Papra, A., et al., *Microfluidic networks made of poly (dimethylsiloxane), Si, and Au coated with polyethylene glycol for patterning proteins onto surfaces.* Langmuir, 2001. **17**(13): p. 4090-4095.

19. Thorsen, T., S.J. Maerkl, and S.R. Quake, *Microfluidic large-scale integration.* Science, 2002. **298**(5593): p. 580.
20. Erickson, D. and D. Li, *Integrated microfluidic devices.* Analytica Chimica Acta, 2004. **507**(1): p. 11-26.
21. Yamada, M. and M. Seki, *Nanoliter-sized liquid dispenser array for multiple biochemical analysis in microfluidic devices.* Analytical chemistry, 2004. **76**(4): p. 895-899.
22. Whitesides, G.M. and A.D. Stroock, *Flexible methods for microfluidics.* Physics Today, 2001. **54**(6): p. 42-48.
23. Ziaie, B., et al., *Hard and soft micromachining for BioMEMS: review of techniques and examples of applications in microfluidics and drug delivery.* Advanced Drug Delivery Reviews, 2004. **56**(2): p. 145-172.
24. Stone, H.A., A.D. Stroock, and A. Ajdari, *Engineering flows in small devices.* Annu. Rev. Fluid Mech., 2004. **36**: p. 381-411.
25. Liu, R.H., et al., *Self-contained, fully integrated biochip for sample preparation, polymerase chain reaction amplification, and DNA microarray detection.* Analytical chemistry, 2004. **76**(7): p. 1824-1831.
26. Chen, X., et al., *A prototype two-dimensional capillary electrophoresis system fabricated in poly (dimethylsiloxane).* Analytical chemistry, 2002. **74**(8): p. 1772-1778.
27. Webster, A., J. Greenman, and S.J. Haswell, *Development of microfluidic devices for biomedical and clinical application.* Journal of Chemical Technology & Biotechnology.
28. Polacheck, W.J., *Effects of interstitial flow on tumor cell migration.*
29. Lantz, A.W., Y. Bao, and D.W. Armstrong, *Single-cell detection: test of microbial contamination using capillary electrophoresis.* Analytical chemistry, 2007. **79**(4): p. 1720-1724.
30. Squires, T.M. and S.R. Quake, *Microfluidics: Fluid physics at the nanoliter scale.* Reviews of modern physics, 2005. **77**(3): p. 977.
31. Kang, Y. and D. Li, *Electrokinetic motion of particles and cells in microchannels.* Microfluidics and Nanofluidics, 2009. **6**(4): p. 431-460.
32. Zhao, H., *Electro-osmotic flow over a charged superhydrophobic surface.* Physical Review E. **81**(6): p. 066314.
33. Whitesides, G.M., et al., *Soft lithography in biology and biochemistry.* Annual Review of Biomedical Engineering, 2001. **3**(1): p. 335-373.
34. Kane, R.S., et al., *Patterning proteins and cells using soft lithography.* Biomaterials, 1999. **20**(23): p. 2363-76.
35. Goyal, S., *Nannoscale Approaches For Biomolecule Separation And Detection.*
36. Ikada, Y., *Surface modification of polymers for medical applications.* Biomaterials, 1994. **15**(10): p. 725-736.
37. Hatakeyama, H. and T. Hatakeyama, *Interaction between water and hydrophilic polymers* 1.* Thermochimica acta, 1998. **308**(1-2): p. 3-22.
38. Oksanen, C.A. and G. Zografi, *The relationship between the glass transition temperature and water vapor absorption by poly (vinylpyrrolidone).* Pharmaceutical research, 1990. **7**(6): p. 654-657.
39. Allen, T.M., *The use of glycolipids and hydrophilic polymers in avoiding rapid uptake of liposomes by the mononuclear phagocyte system.* Advanced drug delivery reviews, 1994. **13**(3): p. 285-309.
40. Weiss, P., et al., *Injectable bone substitute using a hydrophilic polymer.* Bone, 1999. **25**(2): p. 67S-70S.
41. Mikkelsen, R.L., *Using hydrophilic polymers to control nutrient release.* Nutrient Cycling in Agroecosystems, 1994. **38**(1): p. 53-59.
42. Otsuka, H., Y. Nagasaki, and K. Kataoka, *PEGylated nanoparticles for biological and pharmaceutical applications.* Advanced drug delivery reviews, 2003. **55**(3): p. 403-419.

43. Hirotsu, T., *Water ethanol separation by pervaporation through plasma graft polymerized membranes.* Journal of applied polymer science, 1987. **34**(3): p. 1159-1172.
44. Shah, D., et al., *Pervaporation of alcohol-water and dimethylformamide-water mixtures using hydrophilic zeolite NaA membranes: mechanisms and experimental results.* Journal of Membrane Science, 2000. **179**(1-2): p. 185-205.
45. Tandon, V., et al., *Zeta potential and electroosmotic mobility in microfluidic devices fabricated from hydrophobic polymers: 1. The origins of charge.* Electrophoresis, 2008. **29**(5): p. 1092-1101.
46. Tong, J., C.A. Simmons, and Y. Sun, *Precision patterning of PDMS membranes and applications.* Journal of Micromechanics and Microengineering, 2008. **18**: p. 037004.
47. Weibel, D.B., W.R. DiLuzio, and G.M. Whitesides, *Microfabrication meets microbiology.* Nature Reviews Microbiology, 2007. **5**(3): p. 209-218.
48. Hillborg, H., et al., *Crosslinked polydimethylsiloxane exposed to oxygen plasma studied by neutron reflectometry and other surface specific techniques.* Polymer, 2000. **41**(18): p. 6851-6863.
49. Chandler, D., *Interfaces and the driving force of hydrophobic assembly.* Nature, 2005. **437**(7059): p. 640-647.
50. Lum, K., D. Chandler, and J.D. Weeks, *Hydrophobicity at small and large length scales.* The Journal of Physical Chemistry B, 1999. **103**(22): p. 4570-4577.
51. Van Oss, C.J. and R.F. Giese, *The hydrophilicity and hydrophobicity of clay minerals.* Clays and Clay Minerals, 1995. **43**: p. 474-477.
52. Silverstein, K.A.T., A.D.J. Haymet, and K.A. Dill, *A simple model of water and the hydrophobic effect.* Journal of the American Chemical Society, 1998. **120**(13): p. 3166-3175.
53. Gonçalves, P.F.B. and H. Stassen, *Calculation of the free energy of solvation from molecular dynamics simulations.* Pure and applied chemistry, 2004. **76**(1): p. 231-240.
54. Ebenda, J., *POLYMERIZABILITY OF LACTAMS.*
55. Callen, H.B., *Thermodynamics and an Introduction to Thermostatistics.* Thermodynamics and an Introduction to Thermostatistics, 2nd Edition, by Herbert B. Callen, pp. 512. ISBN 0-471-86256-8. Wiley-VCH, August 1985., 1985. **1**.
56. Marcus, Y., *Thermodynamics of solvation of ions. Part 5.—Gibbs free energy of hydration at 298.15 K.* J. Chem. Soc., Faraday Trans., 1991. **87**(18): p. 2995-2999.
57. Beck, C. and F. Schlögl, *Thermodynamics of chaotic systems: an introduction*. Vol. 4. 1995: Cambridge Univ Pr.
58. Devanand, K. and J.C. Selser, *Polyethylene oxide does not necessarily aggregate in water.* Nature, 1990. **343**(6260): p. 739-741.
59. Apicella, A., et al., *Poly (ethylene oxide)(PEO) and different molecular weight PEO blends monolithic devices for drug release.* Biomaterials, 1993. **14**(2): p. 83-90.
60. Peppas, N.A., et al., *Poly (ethylene glycol)-containing hydrogels in drug delivery.* Journal of controlled release, 1999. **62**(1-2): p. 81-87.
61. Merrill, E.W. and C. Sung, *A study of polyethylene oxide-polysiloxane networks as biomaterials for drug release*. 1988, Massachusetts Institute of Technology.
62. Efimenko, K., W.E. Wallace, and J. Genzer, *Surface modification of Sylgard-184 poly (dimethyl siloxane) networks by ultraviolet and ultraviolet/ozone treatment.* Journal of Colloid and Interface Science, 2002. **254**(2): p. 306-315.
63. Dollase, T., et al., *Crystallization of PDMS: The effect of physical and chemical crosslinks.* EPL (Europhysics Letters), 2002. **60**: p. 390.
64. Wong, I. and C.M. Ho, *Surface molecular property modifications for poly (dimethylsiloxane)(PDMS) based microfluidic devices.* Microfluidics and nanofluidics, 2009. **7**(3): p. 291-306.

65. Chen, H., et al., *Surface properties of PEO-silicone composites: Reducing protein adsorption.* Journal of Biomaterials Science, Polymer Edition, 2005. **16**(4): p. 531-548.
66. Liu, V.A., W.E. Jastromb, and S.N. Bhatia, *Engineering protein and cell adhesivity using PEO terminated triblock polymers.* Journal of biomedical materials research, 2002. **60**(1): p. 126-134.
67. Yu, K. and Y. Han, *A stable PEO-tethered PDMS surface having controllable wetting property by a swelling–deswelling process.* Soft Matter, 2006. **2**(8): p. 705-709.
68. Drummond, C.J. and D.Y.C. Chan, *van der Waals interaction, surface free energies, and contact angles: dispersive polymers and liquids.* Langmuir, 1997. **13**(14): p. 3890-3895.
69. Dainton, F.S. and K.J. Ivin, *Changes of entropy and heat content during polymerization.* Transactions of the Faraday Society, 1950. **46**: p. 331-348.
70. Israelachvili, J., *The different faces of poly (ethylene glycol).* Proceedings of the National Academy of Sciences of the United States of America, 1997. **94**(16): p. 8378.
71. Dai, S. and K.C. Tam, *Effect of cosolvents on the binding interaction between poly (ethylene oxide) and sodium dodecyl sulfate.* The Journal of Physical Chemistry B, 2006. **110**(42): p. 20794-20800.
72. Voet, D., *Voet and Voet (1990) Biochemistry*. 1990, Wiley (New York).
73. Lowe, C.R. and P.D.G. Dean, *Affinity chromatography*. 1974: John Wiley & Sons, Ltd.
74. Cuatrecasas, P., *Protein purification by affinity chromatography.* Journal of Biological Chemistry, 1970. **245**(12): p. 3059.
75. Scopes, R.K., *Protein purification: principles and practice*. 1994: Springer.
76. Yamamoto, T., T. Fujii, and T. Nojima, *PDMS–glass hybrid microreactor array with embedded temperature control device. Application to cell-free protein synthesis.* Lab Chip, 2002. **2**(4): p. 197-202.
77. Fujii, T., *PDMS-based microfluidic devices for biomedical applications.* Microelectronic Engineering, 2002. **61**: p. 907-914.
78. Pries, A.R., T.W. Secomb, and P. Gaehtgens, *Biophysical aspects of blood flow in the microvasculature.* Cardiovascular research, 1996. **32**(4): p. 654.
79. Jain, R.K., *Determinants of tumor blood flow: a review.* Cancer research, 1988. **48**(10): p. 2641.
80. Fiddes, L.K., et al., *A circular cross-section PDMS microfluidics system for replication of cardiovascular flow conditions.* Biomaterials. **31**(13): p. 3459-3464.
81. Abdelgawad, M., et al., *A fast and simple method to fabricate circular microchannels in polydimethylsiloxane (PDMS).* Lab Chip.
82. Gabriele, S., et al. *Microfluidic Modeling of Circulating Leukocyte Deformation*. 2009: Springer.
83. Shelby, J.P., et al., *A microfluidic model for single-cell capillary obstruction by Plasmodium falciparum-infected erythrocytes.* Proceedings of the National Academy of Sciences of the United States of America, 2003. **100**(25): p. 14618.
84. Blattert, C., et al. *Microfluidic blood/plasma separation unit based on microchannel bend structures*: IEEE.

BIOGRAPHICAL INFORMATION

Jeyantt Srinivas Sankaran hails from Chennai, a metropolitan city in the southern part of India. He acquired is bachelor's degree in engineering from Velammal Engineering College, Anna University in 2009. His degree was in electronics and instrumentation engineering, with a focus on control systems, specifically distributed control systems.

He joined the Department of Electrical Engineering, University of Texas at Arlington in Fall 2009. Inspired by the work of Dr. Samir Iqbal and several illuminating conversations he joined the Nano Bio Lab in spring 2010. His work has been on multifaceted covering several aspects of physics, chemistry and polymer microfluidics. He also assisted projects involving fabrication of biomimetic scaffolds. He aspires to continue in academia by pursuing a doctoral degree in Electrical Engineering.